

Review

Optical and Physical Applications of Photocontrollable Materials: Azobenzene-Containing and Liquid Crystalline Polymers

Akira Emoto *, Emi Uchida and Takashi Fukuda

Electronics and Photonics Research Institute, National Institute of Advanced Industrial Science and Technology (AIST), 1-1-1 Higashi, Tsukuba, Ibaraki 305-8565, Japan;

E-Mails: emi-uchida@aist.go.jp (E.U.); t-fukuda@aist.go.jp (T.F.)

* Author to whom correspondence should be addressed; E-Mail: akira-emoto@aist.go.jp;
Tel.: +81-29-861-4715.

Received: 5 December 2011; in revised form: 28 December 2011 / Accepted: 7 January 2012 /

Published: 9 January 2012

Abstract: Photocontrol of molecular alignment is an exceptionally-intelligent and useful strategy. It enables us to control optical coefficients, peripheral molecular alignments, surface relief structure, and actuation of substances by means of photoirradiation. Azobenzene-containing polymers and functionalized liquid crystalline polymers are well-known photocontrollable materials. In this paper, we introduce recent applications of these materials in the fields of mechanics, self-organized structuring, mass transport, optics, and photonics. The concepts in each application are explained based on the mechanisms of photocontrol. The interesting natures of the photocontrollable materials and the conceptual applications will stimulate novel ideas for future research and development in this field.

Keywords: azobenzene-containing polymer; liquid crystalline polymer; photocontrol; molecular alignment

1. Introduction

When certain molecules are aligned uniformly, their properties can be tremendously different from those of the corresponding unaligned material. A typical instance is the aligned aramid fibers used as reinforcements in high strength applications, where the regular molecular alignment generates incredible physical properties. The chiral phase in nematic liquid crystal materials is another typical example—when the helical pitch is smaller than the wavelengths of light in the visible region, sharp

selective reflections are generated, which can be observed as brilliant structural colors. The effects of molecular alignment have been used in many fields.

Physical approaches, such as elongation, rubbing, and shearing, are commonly used to produce molecular alignment. These approaches are suitable for homogenous distribution of the alignment. On the other hand, spatial modulation of molecular alignment is also important for advanced applications. Photocontrol is one way of achieving this. Because optical irradiation can be controlled spatially, the spatial molecular alignment can be controlled. If the controllable materials are polymers, the molecular direction is sustained by the backbones. The chemical structure can also be modified by attaching functional moieties. Polymers are also preferable from the viewpoint of compatibility with recent trends flexible and printable electronics.

Over the past several decades, rapid progress have been made in the synthesis, functional design, and application of photocontrollable polymers [1,2]. Azobenzene-containing polymers are typical photocontrollable materials. Linearly-polarized light makes the molecules align in the direction perpendicular to the light polarization, via photoisomerization of the azobenzene [3]. Nowadays, the mechanism is used in various fields. In this paper, we introduce and discuss optical and physical applications of photocontrollable polymer materials, mostly azobenzene-containing polymers and functionalized liquid crystalline polymers. Axis-selective photoreaction can be induced in these materials by irradiation with polarized light, leading to molecular alignment. This property can be built into more functional systems to realize novel concepts. In the review, we summarize the trends in each of the following application areas: photomechanical effects, photonic crystals, diffractive optical elements, relief formation, self-organized structures, and photoinduced chirality. In addition, miscellaneous interesting studies are reported in the “Other applications” section, and the review concludes with a final summary.

2. Photomechanical Effects

2.1. Photo-Actuator

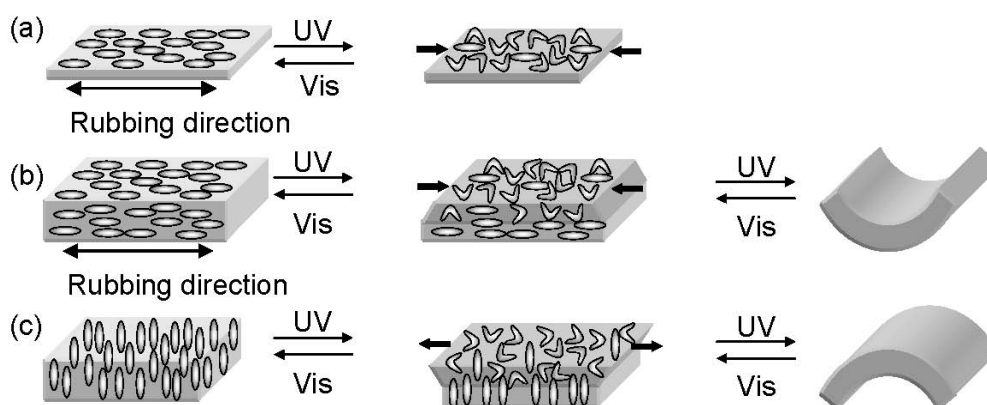
In recent years, a photodeformable material has been developed and attracted considerable attention [4–6]. Macroscopic photoinduced deformation essentially originates in the phototriggered microscopic change of the molecular structure. Since such a material can transform light energy into mechanical energy, application as a photoactuator is expected. Research reports have been presented for both photoisomerizable and photocrosslinkable molecules. Azobenzene [7–9], diarylethene [10] and spiropyran [11] are examples of photoisomerizable molecules, while anthracene [12,13] is a photocrosslinkable molecule. In this section, azobenzene polymers that show macroscopic changes upon exposure to light are introduced.

Eisenbach and coworkers were the first to report that expansion and contraction of an azobenzene elastomer can be reversibly induced by light excitation [14]. Azobenzenes are unique photochromic molecules that reversibly change their molecular shape from a rod-like *trans*-form to a bent *cis*-form upon ultraviolet (UV) light irradiation, and then relax back to the *trans*-form from the *cis*-form upon visible light irradiation. The transformation from *cis*- to *trans*-forms is also induced thermally. Such

molecular photoisomerization may manifest as a macroscopic volumetric change of the whole bulk under appropriate conditions.

Finkelman and coworkers reported that large contraction (shrinkage ratio of about 20%) could be induced in the azobenzene liquid crystalline elastomer [15]. The liquid crystalline nature can decrease the response time for macroscopic deformation, since the molecular response is amplified because of the spontaneous alignment and cooperative motion of the molecules. The direction of the film shrinkage coincides with the alignment direction of the azobenzene molecules obtained by rubbing or film stretching treatment (Figure 1(a)).

Figure 1. Schematic figure of phototriggered film bending in (a) homogeneously aligned thin film, (b) homogeneously and (c) homeotropically aligned thick film, respectively. Irradiation is applied from the top of the films.



Ikeda and coworkers demonstrated that a bending motion of the liquid crystalline azobenzene elastomer was possible [16]. As shown schematically in Figure 1(b,c), they employed thick films, so that the UV light did not penetrate to the back of the film. In some cases, the molecules were initially aligned by rubbing. Photoisomerization of the azobenzene molecules occurs only near the film surface at the incident light side. This photodriven shrinkage or expansion of the surface of the film then results in the bending motion.

The film homogeneously aligned by rubbing bends toward the UV irradiation because of shrinkage of the surface of the film [17] (Figure 1(b)). On the other hand, in the homeotropically aligned liquid crystalline azobenzene thick film, photodriven isotropic expansion occurs only near the film surface at the light incident side upon irradiation with UV light. Then, the film bends away from the UV light source [18] (Figure 1(c)). The bent film returns to its original state upon irradiating with visible light. These anisotropic bending and unbending states can be repeated. The bending direction relative to the incident light can be controlled by changing the alignment of the liquid crystalline molecules.

Broer and coworkers reported that the response time and the degree of bending motion could be improved by employing a hybrid alignment structure for the film [19]. The molecular alignment in the hybrid film changes along the thickness. The molecules of the side of the film nearest the incident light are aligned homogeneously, while the opposite side of the film has homeotropic alignment. Also, in the hybrid film, the concentration of the azobenzene moieties was adjusted so that the excitation light can penetrate to the back of the film. Then, the photodriven bending motion improves as the incident side shrinks and the opposite side expands.

Moreover, it has been demonstrated that the bending direction can be controlled by excitation with linearly polarized UV light [20]. The targeted material was a liquid crystalline azobenzene elastomer film with polydomain structure. In this film, the specific domain, whose alignment direction coincides with the polarization direction of the excitation light, is able to selectively photoisomerize and bend depending on the direction of the light polarization.

Photodriven deformation can be observed in fibers [21] of the liquid crystalline azobenzene elastomer via the same mechanism. If a thermally liquefied liquid crystalline azobenzene elastomer is stretched to produce a fiber, the azobenzene molecules align along the direction of the long axis of the fiber. Thus, the bending direction of the fiber can be controlled arbitrarily depending on the incidence of the excitation light. The application of the photodriven deformation of particles for photonic crystals will be introduced in the Section 3.1.

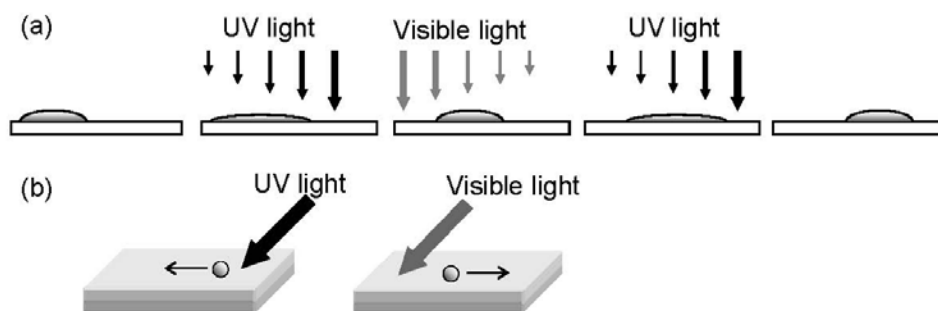
Very recently, research has extended from investigations of reversible bending motion to translational [22,23] or rotational motions [24]. Applications as an artificial muscle and an optical plastic motor [24] are in progress. From now on, the applications for photodeformable materials will continue to develop further, as long as progress continues to be made in large-scale synthesis and processing, durability improvement and efficiency. For example, remote control of a power transmission device for special situations may be possible in the future.

2.2. Photomanipulation

In this section, moving and rotating minute objects by optical manipulation through the reversible change in physical properties of the azobenzene molecule will be introduced.

Ichimura and coworkers have reported the optical control of a water droplet on a substrate whose surface is functionalized by a calix-resorcinarene derivative bearing an azobenzene moiety [25,26]. The phenomenon is based on a reversible wettability change of the film surface through the photoisomerization of the azobenzene moiety. When the surface is irradiated with a graded light pattern, a spatial distribution of wettability is produced on the film surface (Figure 2(a)). Then the droplet is dragged according to this wettability gradient. The direction of motion and the speed are tunable by the direction and power distribution of the excitation light.

Figure 2. Light-driven motion of (a) liquids on a photoresponsive surface consisting of a calix-resorcinarene derivative bearing azobenzene and (b) a solid particle on the surface of a liquid crystalline film doped with an azobenzene derivative.



There are also reports on the movement of an oil droplet floating on the water surface [25,27]. A cationic azobenzene surfactant was dissolved in water. Upon irradiation, the interfacial tension changes since the photoisomerization of the azobenzene derivative takes place. In contrast to the *trans*-form of the azobenzene, the *cis*-form exhibits rather high surface tension. The *cis*- and the *trans*-forms can be preferentially generated by UV and visible light irradiation, respectively. By partial light irradiation of the droplet, a distribution of interfacial tension is induced and convection inside the droplet is generated. It is considered that this convection is a driving force for movement of the oil droplet. The direction of the movement is also defined by the wavelength of the excitation light. The droplet moves so that it escapes from incident UV light, but it is drawn to incident visible light. The direction and the speed of the movement are controllable by the irradiation position and intensity of excitation light. Moreover, simultaneous irradiation with UV and visible sources results in stable trapping of the oil droplet.

There are also reports on control of the arrangement and motion of other minute objects, such as a micro droplet, polymer particles or a glass rod suspended in a nematic liquid crystal doped with azobenzene derivatives. The droplets and particles suspended in the nematic liquid crystal reveal interesting properties as a result of their interaction with the liquid crystal [28–30]. Lev and coworkers reported self-organized structure formation by tailored droplets or poly(methyl methacrylate) particles in nematic liquid crystal colloids [28]. Based on their report, Yokoyama and coworkers succeeded in photoinduced manipulation of dispersions of glycerol droplets suspended in a nematic liquid crystal doped with azobenzene derivatives [31]. The photodriven motion was attributed to the change of tension at the droplet-liquid crystal interface due to photoisomerization of azobenzene. The phenomenon is expected to be applicable for fabrication of photonic crystal circuits or array-based bio-assay devices.

More recently, research concerning the photocontrolled manipulation of microscale solid objects on the surface of a film of liquid crystal doped with a chiral azobenzene compound has been reported by Kurihara and coworkers [32,33]. Translational motion of a microscale object was observed in the racemic system (nematic liquid crystal doped with a racemic azobenzene compound or compensated nematic liquid crystal with cholesteric liquid crystal and chiral azobenzene compound) (Figure 2(b)). The direction of the translational motion was controllable depending on the irradiation position. In the case of the chiral system, rotational manipulation of the microscale glass rod was observed, instead of the translation motion observed in the cholesteric liquid crystal doped with the chiral azobenzene compound. The direction of the rotation was changed by changing the handedness of the system or by changing the wavelength of the irradiating light from UV to visible. They suggested that the phenomenon may also be applicable for biological materials such as DNA, RNA, or bacteria, and other nanoparticles.

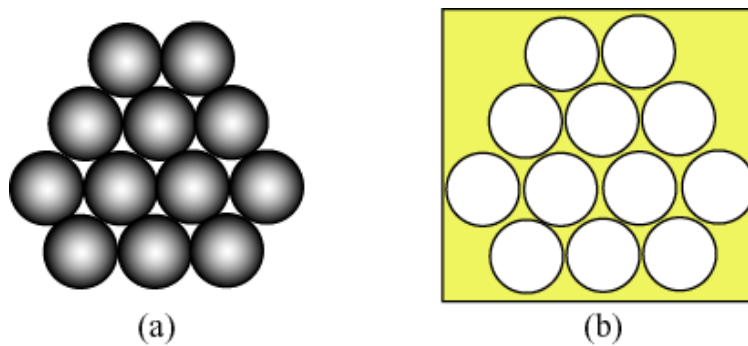
If the optically fabricated or arranged structure in fluids can then be fixed by some appropriate process such as photopolymerization, applications for micro-optics or bioanalytic devices would become more feasible. Further development of other related technologies is also expected.

3. Photonic Crystals

3.1. Colloidal Crystals

Since the concept of photonic crystals was presented by Yablonovitch in 1980s [34], it is one of the most important subjects in photonics and remains so today. The forbidden band within optical region of the electro-magnetic waves attracts attention to the developments of photonic devices. A feasible route to obtain three-dimensional photonic crystals is to use self-assembling of colloidal spheres [35]. The self-organized formation creates photonic crystals almost automatically. We can easily estimate the forbidden band in the visible region, from the brilliant structural colors [36]. The colloidal crystal has two types of structures, opal and inverse opal [37], as shown in Figure 3.

Figure 3. Two types of colloidal crystals, (a) opal and (b) inverse opal.



In the case of opal, the spheres are the substance and the voids are filled by air, while for inverse opal, the spherical parts are filled by air, and residual part is formed by the matrix. Introduction of photocontrollable materials into this system is of interest. At present, both opals and inverse opals can be made from azobenzene-containing polymer materials. The aim of the development of photonic crystals formed by photocontrollable polymers is to be able to tune the photonic band based on the modification of the refractive index contrast, as a result of photoirradiation. These active photonic crystals could be used as future photonic devices.

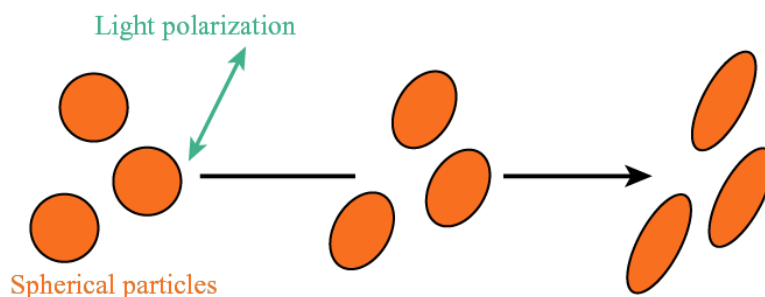
Kurihara and coworkers fabricated colloidal crystals by infiltration of azobenzene liquid crystalline polymer (Azo-LCP) into a SiO_2 inverse opal structure while heating to give isotropic phase and fluidity [38,39]. A spherical structure of Azo-LCP with diameter of 300 nm in a crystal array was achieved. The colloidal crystal was irradiated for several tens of minutes with a variously polarized light of wavelength 488 nm emitted from an Ar^+ laser. In the experiments, a shift of more than 15 nm in the peak of the reflection spectrum was achieved. This indicates that photonic band tuning can be induced by light using photocontrollable polymers. Because of the thermal properties of the Azo-LCP, the response time is relatively long. Although the problem can be improved by operating at high temperatures, the relaxation of the molecules became pronounced [40]. They reported other Azo-LCP to improve the spectral shift, in which azobenzene and tolane mesogens are copolymerized in the side chain of Azo-LCP [41]. As a result, the refractive index change increased under irradiation, and a shift in the spectral maximum of more than 55 nm was achieved.

The inverse opal structure can be also fabricated from a photocontrollable polymer as reported by Kim and coworkers [42]. Silica colloidal crystals were infiltrated with a solution of azopolymer

(poly(disperse orange 3)), and the solvent was evaporated. The infiltrated opal and the inverse opal prepared by removal of the silica spheres via an etching process were fabricated and their grating constants were about 700 nm. Their spectral shifts upon irradiation with Ar⁺ laser (wavelength 488 nm) were measured. Shift of 40 nm and 20 nm were achieved for the infiltrated opal and the inverse opal, respectively, thus showing that the photonic band of an inverse opal can be tuned via refractive index changes.

In a more direct approach, the spherical particles themselves were made from azopolymers. Wang and coworkers fabricated colloidal particles with a diameter of about 200 nm through gradual hydrophobic aggregation of amphiphilic azocopolymer [43,44]. In the scanning electron microscope image, a highly ordered two-dimensional colloidal array was found. The spheres were irradiated with a linearly-polarized Ar⁺ laser beam (wavelength 488 nm), and the photoinduced anisotropy was estimated through measurements of the absorption spectra in the direction parallel and perpendicular to the light polarization. The orientation order parameter reached 0.09. They also fabricated colloidal particles from an epoxy-based azopolymer [45–47]. Interestingly, the spherical particles deformed under irradiation with a linearly-polarized Ar⁺ laser beam. The particles were elongated in the direction parallel to the light polarization, as shown in Figure 4. With increasing the exposure energy and/or increasing the degree of functionalization in the polymer, the degree of elongation also increased. This is an example of anisotropic changes in optical constants and physical form, which may find uses in advanced applications.

Figure 4. Deformation of azo polymer colloidal particles.



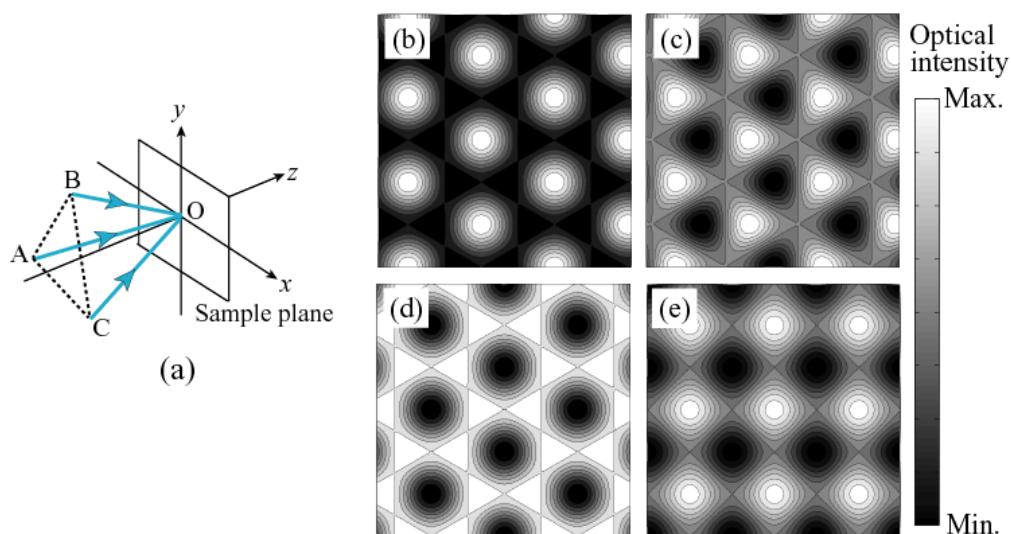
On the other hand, Asher and coworkers developed photo-responsive colloidal crystals composed by hydrogel network possessing azobenzene moieties [48,49]. The diffraction peak switched upon irradiations with UV or visible light. Photonic crystal structures for photonic band tuning have been investigated in other systems including low-molar-mass azobenzene, and spiropyran [50–54]. Based on these rapid advances, realization of high-performance active photonic crystals can be expected.

3.2. Holographic Fabrications

Holographic lithography is also a technique that can be used to fabricate photonic crystal structures. Multi-beam interference field creates various optical intensity distributions, which are determined by the number of beams, their crossing angles, and the amplitude and phase of the beams (*i.e.*, their polarization states). This is based on crystallography, because the interference fringe corresponds to the lattice of a crystal. To create a two-dimensional “crystal structure” of optical intensity, three beams must interfere [55]. For three-dimensional structure, four beams are required [56]. Various interference

patterns can be obtained using three-beam interference, as shown in Figure 5. Holographic lithography is used for photopolymerizable materials. A monomer base mixture is exposed to the interference pattern, and then photopolymerization progresses in the bright regions. After washing out of un-exposed monomers and/or residues, the refractive index contrast between polymer and air results in a photonic crystal.

Figure 5. Typical interference patterns using three beams. (a) Optical arrangement; (b) hexagonal; (c) triangular; (d) inversed hexagonal; and (e) rectangular intensity distributions.



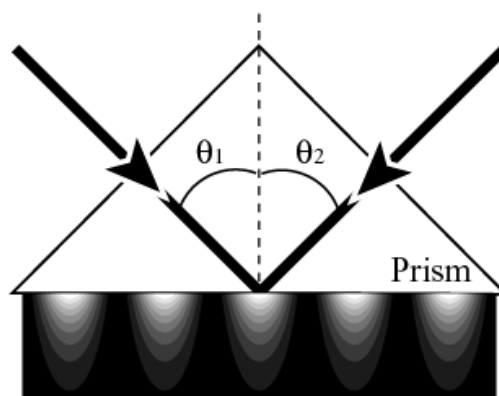
A photocontrollable material was employed to create a tunable photonic crystal [57] using this lithography technique, although the azobenzene used in this particular study was not covalently attached to the polymer matrix. By irradiation with a green laser, anisotropic changes in diffraction efficiency were observed.

Two-dimensional photonic crystals with optical anisotropy based on molecular alignment caused by the polarization modulation of interference fields were demonstrated using photo-crosslinkable liquid crystalline polymers. Ono and coworkers reported both optical properties and theoretical treatment [58,59]. The side-chain type LCP has a cinnamic moiety in its terminal region [60,61]. Under linearly-polarized UV light, the cinnamic parts parallel to the polarization were activated and crosslinked with similarly activated molecules. Subsequently, self-organized reorientation of the non-crosslinked molecules along the axis determined by the crosslinked groups is induced by annealing at its LC temperature (~ 150 °C) resulting in the nematic phase. After cooling, the molecular alignment is stable. Through this mechanism, the LCP can be photocontrolled. Resultant birefringence was estimated to be about 0.2 due to the LC-molecular reorientation. The diffraction characteristics produced by three-beam holography depend strongly on the incident polarization of the probe beam. These diffraction characteristics have been explained by diffraction theory taking into account the anisotropic refractive index changes resulting from the molecular reorientation.

To obtain a subwavelength structure by means of holography using visible light, the crossing angle has to be set to a large value. Ikeda and coworkers reported holographic gratings with subwavelength periodicity in Azo-LCP films [62]. Although the relief depth remained less than 10 nm, both surface

volume changes and refractive index changes resulting from molecular orientation were clearly found in the experiments. On the other hand, evanescent wave interference has also been reported [63] for fabricating subwavelength gratings. A simple setup in Figure 6; the interference field penetrates into a photoresponsive film from the interface between the prism and film. The length of penetration is known to be of similar scale to the wavelength. The interference fringe formed by the evanescent waves from two-beam incidence is determined by the crossing conditions [64]. This technique has been expanded into polarization holography in azopolymer films [65]. Ohdaira and coworkers observed relief formation of azobenzene molecules by evanescent wave interference in an advanced arrangement embedded in an atomic force microscope [66]. A grating periodicity of about 200 nm was clearly observed.

Figure 6. Optical arrangement for evanescent interference irradiation.



A lamination process using azopolymer relief gratings and spacer polymer layers has been developed [67]. The diffraction patterns from the layer-by-layer structures indicated that the structures have regulated three-dimensional periodicity.

Progress is being made in holographic techniques in both optical and photonic fields, as mentioned above. By combining with molecular-alignment, novel photonic structures and functional devices may be created.

4. Diffractive Optical Elements

4.1. Anisotropic Gratings

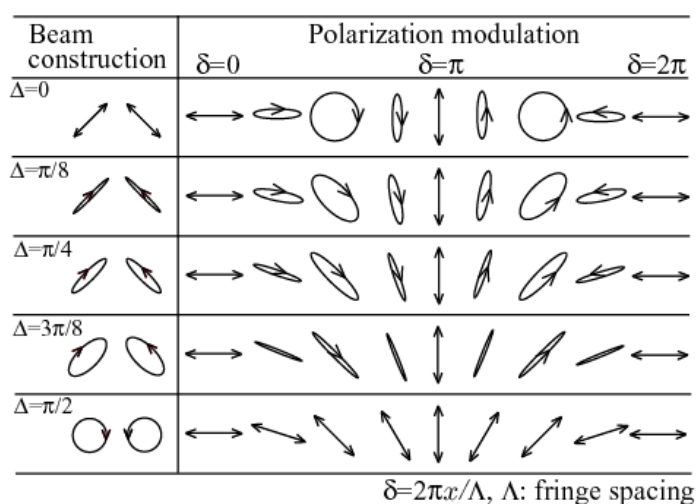
Diffractive gratings with anisotropic refractive index modulations can be formed by polarization holography, which has been well described in a book by Nikolova and Ramnujam that focuses mainly on polarization holography experiments in azobenzene-containing materials [68]. The principles, many experiments, theoretical treatments, and applications are explained in the literature. In this section, we discuss other systems or approaches, including simulation technologies for anisotropic gratings.

Pulsed lasers are mainly used in the nonlinear optics and photonics fields. They produce pulses of nano-, pico-, or femtoseconds, which cover a broad spectrum and wide fields of applications. These lasers can be also employed for holographic recording using photocontrollable materials. Grating formation in azobenzene-containing polymers could be observed even in short times, as required for recording [69–71]. The short-time photoexcitation also provides benefits for investigating dynamic

physical properties via time-resolved investigations [72,73]. The highly regulated pulse width ensures quantitative investigations.

Polarization holography using two-beams adjusted to orthogonal polarization states is usually performed on photoalignment materials, and has provided much information concerning photoinduced changes in anisotropic refractive index and surface volume, for example. Typical types of polarization holography use combinations of s- and p-polarizations (orthogonal linear polarizations), and left- and right-circular polarizations (orthogonal circular polarizations). Both interference fields have pure polarization modulations without intensity modulations. The other condition for pure polarization modulation, that is, interference of orthogonal elliptic polarizations (as shown in Figure 7), was also investigated with azo-dye doped polymer films [74]. The experimental results were explained by theoretical investigations based on Jones analysis. These results indicated that the polarization states of diffracted beams can be controlled by the choice of ellipticity of the two-writing beams.

Figure 7. Optical arrangement for elliptic polarization interference irradiation. Δ is the phase difference in each elliptic polarization, and x is the lateral axis parallel to the grating vector.



Multiplexed holographic gratings in photocontrollable materials have also been investigated. Angular multiplexed recording is discussed in the following section. Here, we focused on in-plane multiplexed recording, that is, for the cases that use a thin film medium. When relief gratings formed by intensity hologram were inscribed in the azopolymer film, the diffraction characteristics are strongly depend on the polarization direction of the reading beam, and the diffraction efficiency depend on the recording energy and resultant relief depth. Based on these characteristics, in-plane multiplexed high-density optical memory was demonstrated [75]. For multiplexed recording with pure polarization modulation in a photocrosslinkable LCP, multiplexed diffraction of various polarizations was reported. Base on the recording mechanism of the photocrosslinkable LCP [60], each hologram retained the information without crosstalk [76,77].

Among these studies of anisotropic diffractive gratings, theoretical treatments have been investigated [78–80]. Computer simulations have also been advanced. In particular, the finite difference time domain (FDTD) method is widely applied for the optical propagation analysis.

Nowadays, the FDTD method has been expanded to add a vectorial treatment of electrical magnetic field, including the dielectric tensor ϵ :

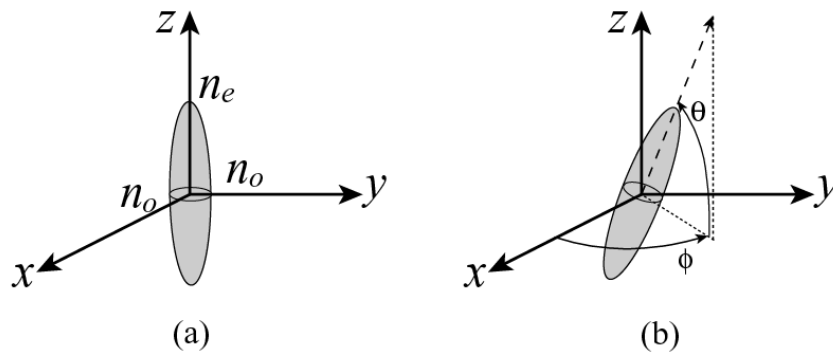
$$\epsilon = \epsilon_0 \begin{bmatrix} \epsilon_{xx} & \epsilon_{xy} & \epsilon_{xz} \\ \epsilon_{yx} & \epsilon_{yy} & \epsilon_{yz} \\ \epsilon_{zx} & \epsilon_{zy} & \epsilon_{zz} \end{bmatrix} \tag{1}$$

where ϵ_0 is the dielectric constant of a vacuum. Considering the uniaxial-molecular alignment from the laboratory coordinate system as shown in Figure 8, the resultant elements of the tensor are written as functions of the slant angles θ and ϕ :

$$\begin{aligned} \epsilon_{xx} &= n_o^2 + (n_e^2 - n_o^2) \cos^2 \theta \cos^2 \phi, \\ \epsilon_{xy} &= \epsilon_{yx} = (n_e^2 - n_o^2) \cos^2 \theta \sin \phi \cos \phi \\ \epsilon_{xz} &= \epsilon_{zx} = (n_e^2 - n_o^2) \sin \theta \cos \theta \cos \phi \\ \epsilon_{yy} &= n_o^2 + (n_e^2 - n_o^2) \cos^2 \theta \sin^2 \phi, \\ \epsilon_{yz} &= \epsilon_{zy} = (n_e^2 - n_o^2) \sin \theta \cos \theta \sin \phi. \\ \epsilon_{zz} &= n_o^2 + (n_e^2 - n_o^2) \sin^2 \theta, \end{aligned} \tag{2}$$

Finally, FDTD analysis is performed using the dielectric tensor. Periodic molecular distribution with uniaxial anisotropy can be placed on the analysis regions. Polarization holograms have been simulated, and these results are consistent to with other theoretical [81,82] and experimental results [83]. The visualized optical propagation obtained from the simulations is especially useful for developments of optical devices. Recently, a flexible fabrication process for anisotropic gratings was developed [84]. Functionally-designed anisotropic gratings will be created by combining with the above simulation technologies.

Figure 8. Uniaxial molecule in the laboratory coordinate system (a), and the slanted state (b). n_o and n_e are the refractive index of the molecule in the ordinary- and extraordinary-directions. ϕ is the angle of n_e from x -axis in the xy plane. θ is the angle between the n_e and the xy plane.



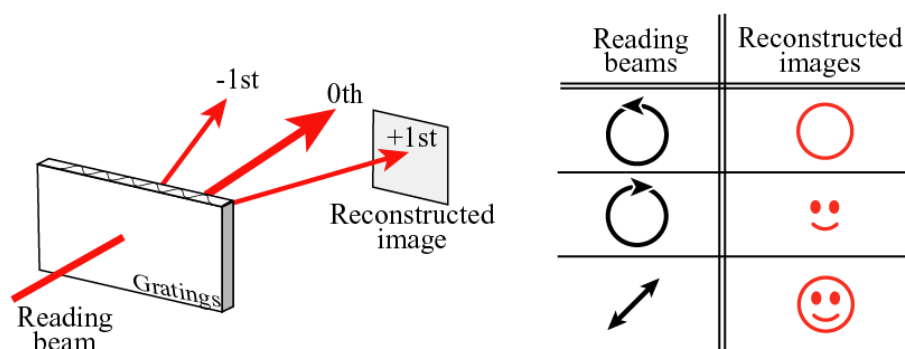
4.2. Applications

In anisotropic diffractive gratings, the diffraction characteristics strongly depend on the polarization states of the incident beams. These gratings have important applications in a wide variety

of fields, including as image holograms, for polarization measurements, information processing, and high-density memory.

If multiple images can be reconstructed within the one hologram, the advantages are invaluable for optical image processing, optical memory, and holographic display technology. In the 1980s, Nikolova and coworkers reported that various anisotropic gratings can be recorded in azopolymer films. In addition, the recorded images can be selectively reconstructed depending on the polarization states used for the recording and reconstruction [85,86]. One of the concepts is illustrated in Figure 9. When a combination of orthogonal circular polarizations is used for hologram recording, the diffraction patterns are completely asymmetric for the circularly-polarized reading beam. This asymmetric diffraction can be observed in the case of a Fourier image hologram [87]. In addition, the asymmetry is inverted by swapping the orthogonal circular polarizations of the two-writing beams. Using these asymmetric diffractions to produce twice multiplexed recording, two recorded images can be selectively reconstructed depending on the rotation direction of the circularly-polarized reading beams. For linearly polarized or elliptically polarized reading beams, two images can be reconstructed simultaneously as shown in Figure 9. In other experiments with photoalignment materials, functional reconstructions of optical images have been reported [88].

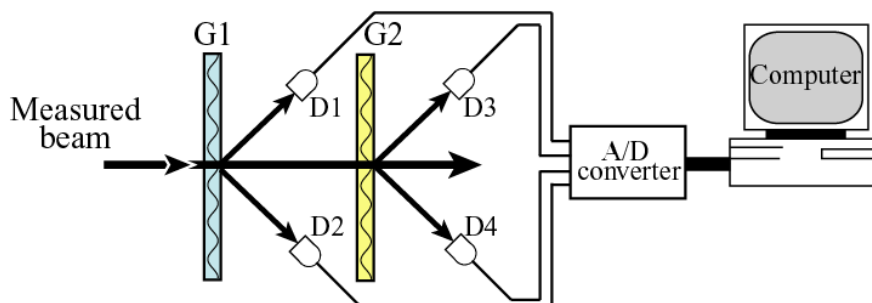
Figure 9. An example of image processing using multiplexed anisotropic grating reconstructions.



A polarimeter (Stokesmeter) system is also a successful application of anisotropic gratings. The fundamental configuration is shown in Figure 10 [89]. The system contains two anisotropic gratings (G1 and G2): one is used for the detection of beam ellipticity and the rotation direction, the other is used for the detection of the polarization azimuth. This is based on the diffraction characteristics being strongly dependent on the incident polarization states in each grating. The polarization state of the incident beam is determined by four diffraction intensities (detected by D1, D2, D3, and D4) through the calculation of each Stokes parameter using a computer. Using the wavelength-dependence of the angular dispersion of diffraction angle, the system was expanded into spectral Stokesmeters [90]. Crossed gratings that include the two gratings for polarization determination have been fabricated in a photocontrollable LCP film [91]. Recently, Cipparrone and coworkers reported the application of anisotropic gratings for a circular dichroism (CD) spectrometer [92]. This new arrangement has a simpler configuration than conventional CD spectrometers. However, azopolymer materials are not suitable for these polarimeter applications because the relief modulation is particularly prominent even in the case of polarization holography. Zhang and coworkers have developed an azopolymer that shows greatly reduced relief formation for the recording of polarization holography [93]. The side-chain

azopolymer is copolymerized with azobenzene moieties and photocrosslinkable moieties. The crosslinking system allows the azopolymer film to form a pure polarization hologram, inhibiting the relief formation.

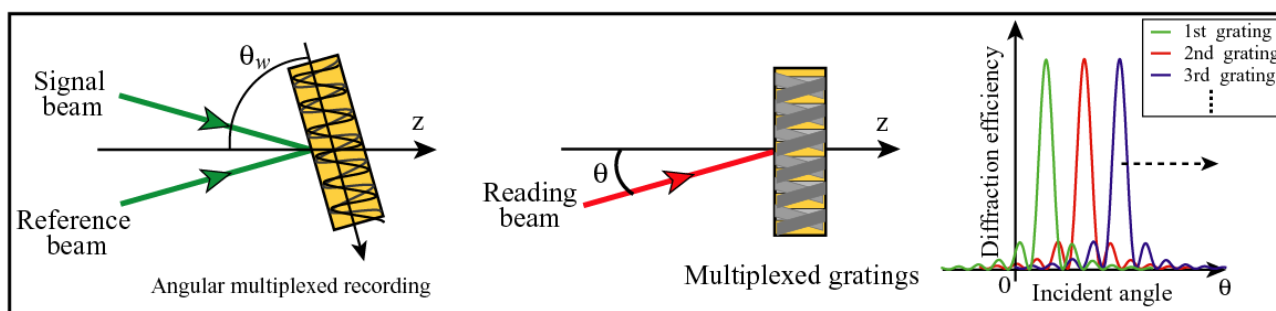
Figure 10. Fundamental configuration of a polarimeter (Stokesmeter) using two anisotropic gratings.



Anisotropic gratings have the function of polarization conversion in the diffracted beams and these typical conversion characteristics can also be found in polarization holography, as well-known [94]. This type of applications is advancing. Specially-designed gratings generate the conversion function such a circularly-polarized incident beam is converted into linearly-polarized beam in the diffracted beams [95]. Similarly, the holographic gratings designed to generate interesting asymmetric diffraction was reported [96]. On the other hand, the diffraction characteristics of anisotropic gratings have also been applied to logic operations with Boolean algebra [97]. Several kinds of logic operation were demonstrated.

Holographic memory is also an important and suitable field for molecular controllable materials. The volume hologram formed in a thick hologram medium is particularly important because it allows us to produce angular-multiplex recording, as shown in Figure 11. By using polarization-sensitive polymer materials, as discussed in this paper, realization of tremendously high-density memory can be expected by the combination of angular multiplexed recording and polarization multiplexed recording. Ramanujam and coworkers reported the potential of photocontrollable (photoaddressable) liquid crystalline polymers for holographic memory [98]. For the combination of chromophore and mesogenic moiety, the importance of the synergistic molecular reorientation was explained. Hvilsted and coworkers reported the volume holographic storage potential in azobenzene containing polymers, including the explicit current issues [99].

Figure 11. Angular multiplexed holographic gratings in a thick medium.



Ikeda and coworkers developed many high performance azobenzene LCPs, such as an azobenzene LCP with azobenzene and biphenyl moieties in the side chains of the copolymer [100]. The combination of angular multiplexed recording and polarization multiplexed recording was clearly demonstrated. When tolane moieties were copolymerized into azobenzene LCPs, large photoinduced refractive index changes were obtained, resulting in high diffraction efficiency [101]. The mesoscopic morphologies created by polymer blends and/or block copolymers and photoalignment molecules are also used for anisotropic recording media. Synergetic effects were present in the holographic recording, leading to improved of diffraction efficiency with optical page data [102], large photo-induced birefringence and hologram stability [103], and achievement of high-density recording and the high-reproducibility in the cyclic recording and erasing process [104].

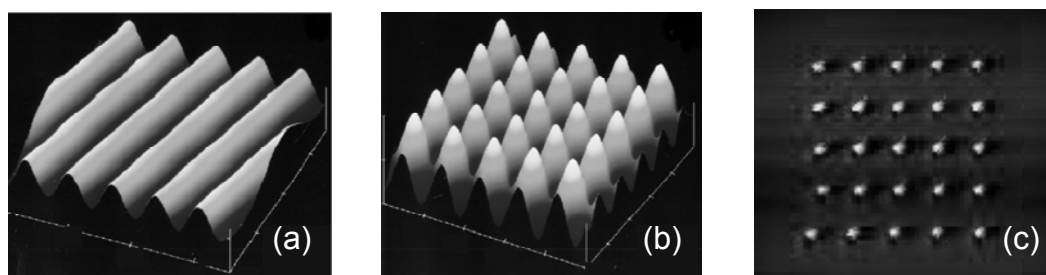
The applications of anisotropic gratings formed by photocontrollable materials are spreading from the initial interest in optics into the field of information technology. Using controlled optical anisotropy, conventional optical elements can be built up into highly functionalized polarization devices.

5. Relief Formation

5.1. Micro- and Nanoscale Formations

Surface relief structures with large amplitude can be fabricated on azobenzene-containing polymer films upon irradiation with green or blue light (Figure 12). This phenomenon is known as photoinduced surface relief (PSR) formation, and intensive studies have been performed since the first report in 1995 [105,106]. PSR formation originates in optically driven large scale mass transport, but does not involve thermal effects, ablation or irreversible photochemical reactions. Thus the process is essentially reversible.

Figure 12. Typical example of PSRs formed by exposure of (a) an interference pattern with 0.6- μm period; (b) orthogonal interference patterns with 1- μm periods; and (c) optical near field emitted from an optical fiber with 30-nm aperture.



The profile of the inscribed PSR structure is determined by the spatial distribution and the polarization condition of the irradiated light pattern [107]. Many models for the PSR mechanism have been proposed so far [108–114].

The PSR structure is very stable unless the films are heated up to their glass transition temperature. An inscribed PSR structure has been shown to be stable for at least 10 years if it kept in laboratory conditions. However, the structure is erasable if the film is heated above its glass transition temperature or irradiated with strong uniform light. Surface modulation through PSR formation can be

achieved on a scale finer than 1 μm at suitable processing conditions. The spatial resolution can be as detailed as few-tens of nm or less. These aspects of the phenomenon are favorable for manufacturing micro- and nanoscale surface structure formations.

The formation of a periodic grating structure through a two-beam interference pattern has been thoroughly studied in the dawn of this research topic. Although a single exposure of the interference pattern gives a sinusoidal surface relief grating, more intricate grating structures can also be inscribed by using multiple exposures. For example, Tripathy and coworkers succeeded in fabricating a beat structure, an egg-crate (orthogonal gratings) structure, a Fourier synthesized blazed grating structure, a hexagonal honeycomb structure and so on [115]. The possibility of superposition of the structure by using multiple exposures is a very unique feature of the PSR phenomenon, which is not observed on conventional photoresists or photopolymers. This characteristic is advantageous for the formation of a complicated structure. Using this method, the spacing of periodic structures can be varied in practice from 0.3 to 50 μm (or more) by just adjusting a coupling angle of the two coherent beams. The PSR inscription rate depends on many experimental parameters such as the value of the spacing, the initial film thickness, and the azobenzene functionalization [116,117].

A distributed fringe structure has been inscribed using a diffraction pattern from a knife edge [105,118]. The pitch of the fringe included in the structure varied from about 10 μm to a submicron. In addition to the continuous structures, a polarization dependent pit structure has been inscribed using a focused Gaussian beam [119]. The diameter of the pits can vary from a few microns to a few tens of microns. The inscription rate of the PSR strongly increases with decreasing diameter of the irradiated Gaussian beam. The fringe and pit structures have both been thought-provoking regarding the origin of the driving force for PSR formation.

An amplitude photomask can also be employed for arbitrary pattern exposure; not only simple geometrical binary patterns, but complex images with gray scales can be inscribed as well [120,121]. Furthermore, PSR structures with dimensions below the optical diffraction limit can be inscribed by exposure of the optical near-field. There are several methods for the generation of an optical near-field. Ikawa and coworkers proposed a method using polystyrene nanospheres and suggested that the spatial resolution obtained by the method is at least 20 nm [122]. Boilot and coworkers and Fukuda and coworkers independently demonstrated that the formation of a nanoscale dot array and nano-characters was possible by a method using an optical fiber with a tiny aperture at the tip [123–125]. Sekkat and coworkers reported a silver-coated tip for an atomic force microscope that can generate an optical near-field spot, and can be used for near-field nanofabrication [126]. Furthermore, Karageorgiev and coworkers reported nano-manipulation by a method using the probe tip of a scanning force microscope. The spatial resolution revealed in their experiment was also about 20 nm [127].

Seki and coworkers investigated a mixture of an azobenzene polymer and a nematic liquid crystal, and reported that the PSR inscription rate during the initial stage was enhanced by more than two orders of magnitude compared with that of typical amorphous azobenzene polymers [128]. This result could be attributed to the characteristics of the lower viscosity and the cooperative molecular motion that were brought by an addition of the liquid crystalline molecule into the system. Although most research on PSR formation has been done on azobenzene amorphous polymer, other systems have been targeted in recent years, such as spiropyran-doped poly(methyl methacrylate) and amorphous hexaarylbiimidazole [129,130].

Since it reduced chemical and energy consumption and toxic emissions in comparison with conventional lithographic methods, PSR formation is an environmentally conscious technology for micro- and nanoscale fabrication. Moreover, the process is quite simple since it requires only light irradiation, and, uniquely, the photofabricated PSR is erasable. PSR applications will extend beyond simple structure formation technology.

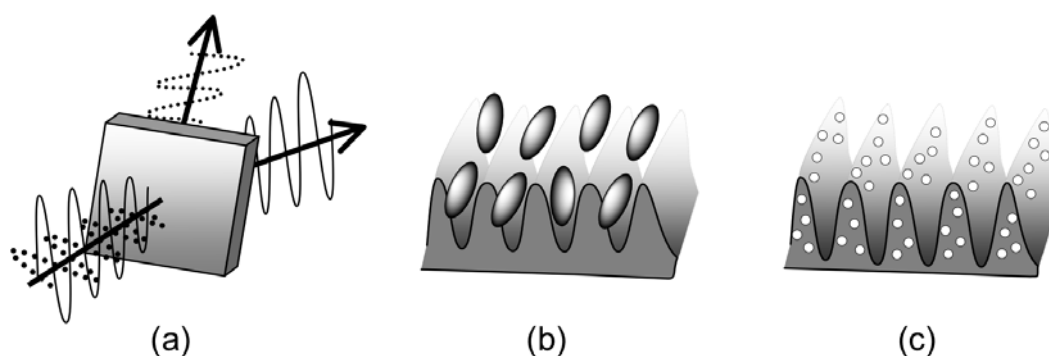
5.2. Applications

Since PSR formation is a facile and effective micro- and nanofabrication process, various applications based on its unique features have been proposed so far. In this section, several photonic, geometric and mechanical applications will be introduced.

The first example is an optical application. PSR structures with submicron or micron periodicity exhibit various useful functions for light modulation (Figure 13(a)). Nathansohn and coworkers proposed a variety of possibilities for the optical application of PSRs, including as grating couplers, narrow band tunable wavelength filters, and polarization separators [131]. Emoto and coworkers demonstrated that asymmetric polarization conversion between +1st and −1st order diffraction beams was possible using a combination of the PSR grating and polarization hologram [96]. Ubukata and coworkers proposed the application of the PSR grating as a waveguide for a distributed feedback laser [132]. They employed malachite green and sulforhodamine as laser dyes, and demonstrated that the lasing wavelength could be tuned by adjusting the period of the rewritable surface relief grating.

Furthermore, as another example of an optical application of the phenomenon of PSR formation, a unique recording method has been proposed for rewritable high-density optical information [75]. By using a PSR structure that consists of a radially located one-dimensional grating in combination with multiple-coding of data, it was proposed that a huge amount of information can be stored. The achieved multi-level data recording density was about 1 GB/inch² using a combination of angular- and depth-gradations with multiplicities of 6 and 4, respectively. The possibility of attaining the recording density of 1 TB/inch² was also suggested.

Figure 13. Schematics of several applications of PSRs (a) optical; (b) geometrical; and (c) mechanical.



The second example covers applications exploiting the geometrical features of the PSR structure. The PSR structure is a facile and effective template for controlling the arrangement of liquid crystal molecules or colloidal spheres (Figure 13(b)). Several research groups investigated the use of

azobenzene polymers with a PSR structure as liquid crystal alignment films. Li and coworkers reported that the PSR structure can tightly anchor the liquid crystal (LC) molecules, and the stability and the transmittance of the PSR/LC assembly could be improved by photobleaching. It is also proposed that this alignment method can be applied to create an in-plane switching device [133–135]. Quantitative examination of the anchoring force associated with the PSR structure has been presented by Chung and coworkers [136]. In addition to alignment control of liquid crystal molecules, investigations on colloidal spheres were performed by some research groups. Ye and coworkers reported that a two-dimensional array of colloidal spheres was obtained by convective self-assembly regulated using a surface relief grating [137]. According to their report, an array with hexagonal symmetry can be obtained when the ratio between the diameter of the sphere and the period of the grating is 1.15 or 2. Under other conditions, the array takes a centered-rectangular symmetry.

Kim and coworkers demonstrated that the PSR structure is also suitable for template-directed alignment of colloidal spheres [138,139]. They suggested that the ratio between the surface modulation and the diameter of the sphere determines the assembled structure. It was reported that three-dimensional square arrays were obtained when the ratio exceeded 0.35. Watanabe and coworkers developed a further technique for colloidal sphere arrangement. They demonstrated that a well-defined two-dimensional array of colloidal spheres can be formed using a PSR template fabricated on an azobenzene polymer film, but furthermore, the arranged spheres can be fixed onto the template by selective photoirradiation [140]. With this technique, area-selective immobilized patterns were obtained after ultrasonication of the sample. The technique is expected to be applied for fabrication of photonic, electronic, and micro-fluidic devices.

PSR structures are useful as facile templates for high-mix low-volume replica production. Fukuda and coworkers achieved at least a hundred times replication using thermosetting resin without any deterioration [141]. The error in the depth of the obtained replicas throughout one hundred times replication was less than $\pm 3\%$. A spatial resolution of the PSR structure replication of better than 300 nm was experimentally confirmed.

The third example is an application for material transfer or patterning based on the mass transfer that occurs during the PSR formation process (Figure 13(c)). Seki and coworkers utilized mass transfer during the PSR formation process to obtain a patterned structure of dichroic dyes or CdSe nanocrystals. They called this technique “phototriggered mass conveyance” [142]. As an example, a mixture of azobenzene polymer, doped with a diaminoanthraquinone-based dye, and nematic liquid crystal was used. In their experiment on this dichroic dye-doped system, macroscopic dichroism was observed. This could be attributed to uniaxial crystal growth initiated by diffusion-limited concentration and aggregation because of the PSR formation. The reported dichroic ratio at the absorption maximum (588 nm) was 6.6. Following a similar concept, patterning of poly(3-dodecylthiophene), a popular p-type organic semiconductor was demonstrated. In their polymer blend system, a liquid crystalline azobenzene polymer was employed as the host material [143]. It is presumed that the phenomenon could not be observed other than the liquid crystalline system since it cannot give sufficient mobility to the conveyable dopant.

In summary, PSR has attracted extensive interest in broad research areas such as optics, physics and chemistry, and various applications have been considered. As elucidation of the mechanisms of the

phenomenon progress, new material development has also advanced. Further development in this area is also anticipated.

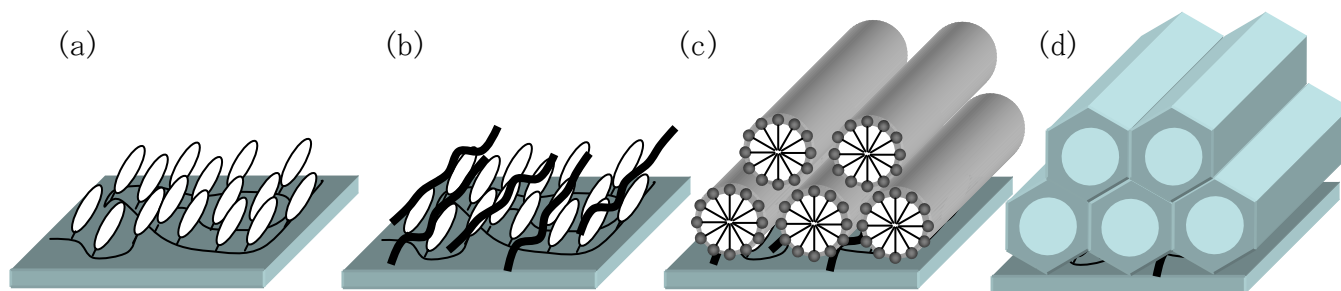
6. Self-Organized Structures

6.1. Mesoporous Structure

With the recent progress in nanotechnology and precision synthesis, nanoporous materials have attracted much attention. A mesoporous material is a three-dimensional nanostructured material with uniform and regular mesoscale (2–50 nm in diameter) fine pores and a surface area of over 1,000 m²/g [144–146]. Because of the extremely large surface area of these materials, several applications are expected—as catalysts, and for adsorption, separation and so on. In recent years, since the successful thin-film fabrication of mesoporous materials, developments have extended to the fields of sensors, separation membranes, photonics [147–149] and electronics [150,151]. It is obvious that alignment of the components may be an effective way to improvement these materials. Thus alignment control of mesoscale fine pores within a macroscopic domain is fundamentally important.

Generally, mesoporous materials are produced by sol-gel processes that used surfactants as molds or templates [145,152,153]. Amphiphilic surfactants assemble spontaneously when dissolved in water if their concentration exceeds the critical micellar concentration. The self-assembled three-dimensional ordered structures exhibit lyotropic liquid crystalline behavior in solution. With increasing surfactant concentration, the self-assembled structure changes from spherical micelle to rod-like micelle and finally to lamellar micelle. After covering the self-assembled surfactant with inorganic oxides such as silica, the material in the form of arranged nanochannels can be obtained by removing the surfactant mold via a sintering or extraction process. The pore size of the fine pores can be controlled by the length of the surfactant. The orientation of the pores directly depends on the self-assembled structure of the surfactant. Uniform alignment of mesoporous silica thin films can be possible under a strong magnetic field or on a rubbed polymer film [154,155]. However, complicated patterning is not simple using these methods.

Ichimura and coworkers reported on controlling the alignment of lyotropic liquid crystalline molecules, by using photoactive surfaces (so-called “command surface”). That paved the way for optical control of nanochannels consisting of mesoporous materials [156]. Seki and coworkers first reported the photo-orientation of a mesostructured surfactant and silica hybrid via hierarchically-relayed multiple transfers among hetero-interfaces [157,158]. The orientation direction was defined by the optically aligned azobenzene monolayer (Figure 14(a)). The mesostructured material was deposited on an alignment film by immersion of the film in the sol-gel reagent [159]. However, direct immersion into a hydrophilic sol-gel reaction solution may induce aggregation of the azobenzene and result in destruction of the molecular orientation since the azobenzene moiety is hydrophobic. To avoid such a problem, they applied a poly(di-n-hexylsilane) thin film onto the oriented azobenzene film. Then the photoinduced anisotropy of the azobenzene film was transferred and fixed in the polysilane layer [160] (Figure 14(b)). Finally, the sol-gel process was completed to obtain a photo-oriented mesoporous silica structure.

Figure 14. Schematic procedure of photoorientation of a mesostructure.

Incorporation of low-molecular weight liquid crystal and dye into the mesochannel was also investigated. The dichroic ratio achieved in this experiment was 0.34 [157]. The same group also reported that photopolymerization of UV-curable liquid crystalline molecules within photoaligned mesoporous silica film produced bundles of nanofibers, and that the molecular weight distribution of the product was rather narrow in comparison with that of the product of bulk photopolymerization [161]. It was suggested that the successful anisotropic incorporation of liquid crystal molecules containing a dichroic dye into the aligned mesochannels may provide new strategies for the creation of hybrid optical devices.

It is also proposed that the photocrosslinkable liquid crystalline polymer [60,162] can be used as an alignment film for fabrication of photo-oriented mesoporous structures. In this method, the proposed alignment layer has sufficient tolerance to immersion in sol-gel reaction solutions, so that no additional intermediate layer is necessary [163]. An additional benefit is that since optical patterning is possible for the photoalignment film, two-dimensional macroscopic patterning of the mesoporous structure is also possible.

The proposed method is a facile and low-cost technology. Thus, it is expected to be a good potential candidate for practical fabrication of mesoporous structures. It is presumed that development of various aspects of the method, such as size control, aspect control, and material composition, will continue. Especially, applications as sensing devices, catalysts and batteries are eagerly anticipated.

6.2. Nano Template

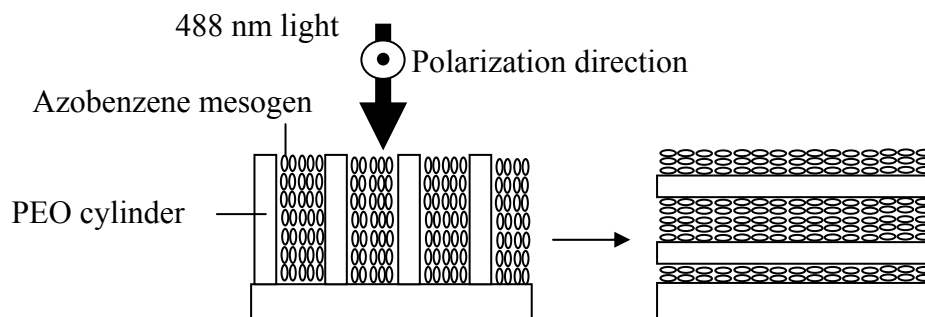
In the previous section, the formation of an oriented nanochannel structure using an optically controlled self-assembled structure formed by amphiphilic low-molecular weight molecules was described. In this section, nano-template fabrication by controlling the self-assembled structure of a block copolymer, and its application will be introduced. The template is considered to be effective for further simplification of nanochannel formation and reduction of product cost.

A block copolymer bearing incompatible segments such as hydrophilic and hydrophobic regions can adopt various self-organized structures such as spherical, lamellar and cylindrical. The self-organized structures are caused by phase separation of the segments. Since the cylindrical structure has a one-dimensional continuous phase, it can be used to create a one-dimensional nanochannel, or even a nano-array by controlling orientation. Lithography using nanophase separation of block copolymers is possible to achieve the processing with higher spatial resolution than conventional beam-based processing technology; thus it has attracted much attention [164].

To control the orientation of the phase separated structure in an amorphous block copolymer, several methods such as using solvent evaporation [165], a magnetic field [166], or an electric field [167] have been reported. However, these methods are not especially efficient; it remains difficult to control the orientation direction. The development of liquid crystalline block copolymers, which mean that orientation control techniques appropriate for liquid crystals can be applied, solved this problem [168,169]. Orientation of the nanocylinder structure can be induced according to the orientation of the liquid crystal molecules. On the other hand, there is also a report that liquid crystalline molecules can be controlled by orientation of the nanocylinder structure in a shear flow field [170]. That is, the orientation of a nanocylinder and a liquid crystal are strongly correlated.

Therefore, orientation of a cylinder is controllable by using photo-orientational control for liquid crystals [171,172]. In a liquid crystalline azobenzene/polyethylene oxide (PEO) block copolymer, Ikeda and coworkers succeeded in controlling the orientation of the PEO cylinder structure by the supramolecular cooperative motions between the ordered azobenzene liquid crystals and PEO cylinder via the polarization of the irradiating light (Figure 15) [171]. Moreover, Seki and coworkers reported photopatterning and alignment of nanocylinders in a hybrid film consisting of a diblock copolymer comprising liquid-crystalline azobenzene and PEO and 4-Cyano-4'-pentylbiphenyl (5CB) by exploiting the process of photoinduced mass migration [172]. Such a film consisting of well-organized PEO domains can be utilized as a nano-template.

Figure 15. Schematic figure of liquid crystal alignment and microphase-separated structures.



Iyoda and coworkers attained uniform alignment in an azobenzene/PEO liquid crystalline diblock copolymer by thermal treatment [173]. The array of hexagonally arranged PEO cylinders is induced by homeotropic alignment of the azobenzene mesogens in the smectic phase. They then succeeded in obtaining complex structural arrangements by selective doping and adsorption of functional materials to PEO cylinder domains exploiting the characteristics of PEO. Some examples are: an array of silica nanorods with mesoporous structure can be formed by selective doping of the silica-sol into the PEO domain [174]; an array of silver nanoparticles can be formed by selective doping with silver cations [175]; and gold nanoparticles can be arranged via selective adsorption to either the hydrophilic PEO domain or hydrophobic mesogenic domain [176]. It is also proposed that this type of nanotemplate can be applicable as a wet etching mask for transferring a nano-pattern onto a silicon wafer [177]. An application as an ion conducting channel has also been suggested [178]. As described in detail in Section 4.2, these block copolymer materials can be applied as optical memory. The unique function given by a combination with photoresponsive and other materials cannot be substituted by other technology. The optically controlled nanostructures are expected to apply for ultra-fine processing

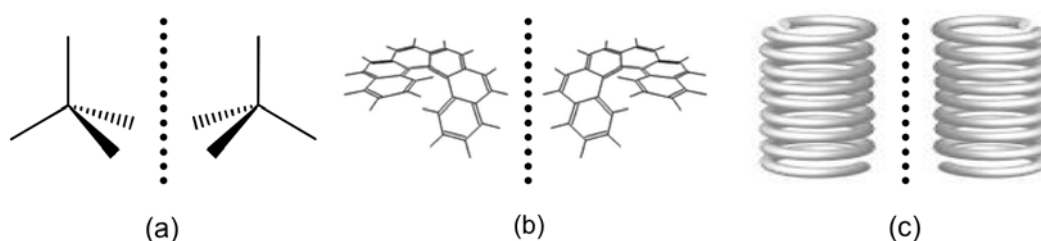
technology exceeding conventional lithography, which will be available for nanophotonics and molecular biology.

7. Photoinduced Chirality

7.1. Chirality Switching and Amplification

Research on the chirality of molecules is of fundamental importance in both industrial and academic chemistry (Figure 16). Much research has recently been reported on the chirality of systems containing photoresponsive molecules, since light is a smart stimulus for inducing molecular arrangement and higher-order structural change in three-dimensional space.

Figure 16. Schematics of (a) molecular chirality; (b) conformational chirality; and (c) supramolecular chirality.



From the point of view of applications of chiroptical properties, liquid crystals and polymers are quite attractive molecular systems. The chiroptical property of a chiral molecule can be remarkably magnified as a result of molecular alignment because of molecular interactions in a liquid crystal or because of the conformation of a polymer chain.

Feringa and coworkers demonstrated that positive and negative cholesteric phases can be recursively generated in a nematic liquid crystalline material containing an inherently asymmetric overcrowded alkene [179]. As the result of an ingenious combination of the CD and the photoisomerization properties of the overcrowded alkene molecules, an efficient deracemization could be achieved depending on the handedness of the circularly polarized excitation light.

Although there are many other reports on chirality switching using deracemization upon circularly polarized light irradiation [180], another interpretation for the deracemization has been proposed by Takezoe and coworkers [181]. Their system consists of W-shaped azobenzene molecule and a nematic liquid crystalline polymer. According to their explanation, the photoinduced chirality upon irradiation with circularly polarized light can be attributed to the lack of equilibrium balance between left- and right-twisted conformations of the azobenzene molecule, which occurs because of the momentum transfer from the light to the molecule. Sierra and coworkers reported that chirality switching can be also induced in a hydrogen bonded complex system that exhibits a columnar liquid crystalline phase [182]. Their system consists of nonmesomeric V-shaped azobenzene arms and melamine derivative core. Oriol and coworkers investigated the photoinduced supramolecular order as a function of the chemical structure of the azobenzene polymer, and discussed it from the viewpoint of the glass transition temperature, the length of the spacer and the nature of the liquid crystalline phase [183]. They reported that a selective reflection was observed in the polymer having a nematic liquid crystalline phase but

not in the polymer having a smectic phase. Considering the most of the all reports concern the nematic phase system, the balance of the local motility of the molecule and the order of the molecular alignment should be an essential point. It can be expected that new findings will continue to emerge on the combination of photoresponsive molecules and liquid crystalline systems.

On the other hand, Zentel and coworkers reported in 1995 that the helicity of the spiral of a polyisocyanate-bearing chiral azobenzene side-chain can be switched through the *trans-cis* photoisomerization of the azobenzene moiety in tetrahydrofuran solution [184]. It is thought that the switching originates in the molecular interaction between the chiral center of the azobenzene side-chain and the polymer main-chain, since it changes depending on the form of the azobenzene photoisomers. From subsequent research based on the same concept, it was reported in 2000 that the phenomenon occurs even in a poly(methyl methacrylate) matrix, and that the photoinduced helical configuration is stable below the glass transition temperature of the matrix [185].

From a practical viewpoint, the discovery of reversible photoswitching of the chiroptical characteristic in the solid state is quite valuable. Pedron and coworkers observed chirality switching in a chiral methacrylate azobenzene polymer [186]. They suggested that the effect might be interpreted as photoinduced inversion of the prevailing helical handedness of the polymeric macromolecules driven by transfer of angular momentum from the circularly polarized light to the azobenzene chromophores. Since the glass transition temperatures of the polymers in their study are rather high (one of the polymers is over 200 °C), superior stability of the photoinduced chirality can be expected. However, the sensitivity needs to be improved further. It was reported that the fluence required for chirality switching is about 10 J·cm⁻¹. Although an improvement in sensitivity of 3 to 4 orders of magnitude is desirable, and may occur via further materials development, there may be a trade-off with the glass transition temperature of the system. In practice, it may be more effective to employ an intense pulsed light for excitation.

In this section, we outlined how photoresponsive molecules can be used to control the chirality in some liquid crystals or polymers and to amplify the molecular chirality by exploiting the macromolecular helical alignment of the system. Over the last decade, research in this field has clearly progressed. In particular, development of a solid state chiral switching material was significant. Further development is also anticipated in the future.

7.2. Supramolecular Chirality

In this section, an example of spontaneous three-dimensional structure formation of achiral photoresponsive molecules upon irradiation with elliptically polarized light will be introduced. Typically this involves the optical formation of a supramolecular helical structure that has a screw axis in the propagation direction of the elliptical polarization. The target material is an achiral photoresponsive polymer having either a liquid crystalline phase or amorphous state. The optical generation of chiral triggers and photoinduced deracemization has already been described in the foregoing sections; such cases are not included in this section.

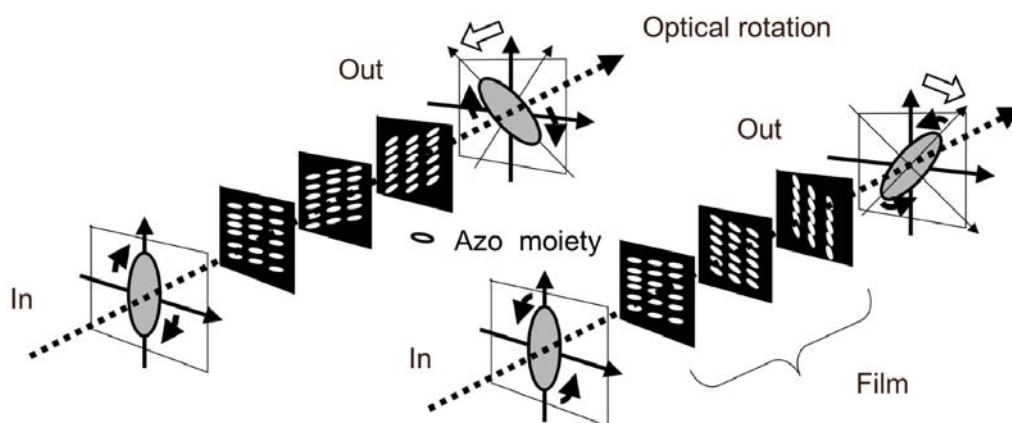
Photoinduced circular anisotropy in a polymer with azobenzene side-chains was first reported by Nikolova and coworkers in 1997 [187]. The degree of photoinduced circular anisotropy was evaluated using linearly polarized light by measuring the rotation of the polarization azimuth; a value of about 6°

per 1- μm -thick film at a wavelength of 488 nm was reported. The value of optical rotation corresponds to a circular birefringence of about 0.01 and reportedly remained stable for months.

Several research groups then extended the research in connection with generation of photoinduced chirality in an achiral azobenzene polymer. Photoinduced circular anisotropy was found to depend on the nature of the excitation light (such as its ellipticity, beam intensity, wavelength and irradiation time) [188–191]. Although the chemical structure of the polymer main-chain employed by each study was different (ester, epoxy, and methacrylate, for example) the proposed mechanism for the generation of the photoinduced chirality was identical. The photoinduced chirality could be attributed to the photofabrication of supramolecular helical alignment of the azobenzene moiety. As shown in Figure 17, the photoinduced chiral structure (helix formation) can arise from the stepwise spontaneous rotation of the optical axis of oriented azobenzene moieties as a result of the propagation of the light.

Nikolova and coworkers reported that the rotation angle depends on the function $\Delta n \cdot e / (1 - e^2)$ [188]. (Here, the terms “ Δn ” and “ e ” represent photoinduced birefringence and ellipticity, respectively.) According to this formula, the degree of photoinduced circular anisotropy should be directly related to the photoinduced birefringence of the material. Based on this concept, an amorphous azobenzene polymer consisting of cyanoazobenzene and a large birefringent bisazobenzene moiety with extended π -conjugation has been developed by Fukuda and coworkers; rotation angles of about 32° and 41° per 1- μm -thick film at wavelengths of 488 and 458 nm, respectively, were reported [191]. The alignment of the azobenzene side-chain in the polymer is robust to thermal relaxation because of the effective molecular interaction between the side-chains; the performance reportedly remained stable for over three years in laboratory conditions. These very large rotation angle values are expected to lead to applications in thin film optical components such as phototunable waveplates (birefringent retarder, optical rotator, *etc.*) and circular dichroic plates [192]. Oriol and coworkers reported on the thermal stabilities of the photoinduced supramolecular chiral structures in nematic and smectic polymers, and concluded that the thermal stability above the glass transition temperature depends on the liquid crystalline nature of the polymer [183].

Figure 17. Schematic illustration of photoinduced supramolecular helical structure formation for (a) left-handed elliptically polarized and (b) right-handed elliptically polarized light, respectively.



Sourisseau and coworkers used Jones' matrix formalism for detailed analysis of photoinduced chirality and concluded that the degree of photoinduced rotation angle can easily be controlled depending on the ellipticity of the excitation light [193]. Based on this characteristic, they suggested that the arbitrary gray level state defined by the elliptical condition of the excitation beam could be potentially interesting for optical data storage or photonic devices. Barada and coworkers demonstrated that optical data could be recorded as a photoinduced chiral structure in an azobenzene amorphous polymer by using elliptically polarized light excitation [194]. In their experiment, the two digital two states of "0" and "1" were defined as the isotropic and photoinduced chiral states, respectively. The possibility of four or more multilevel recording (and reading) was indicated. They mentioned that the reported recording time for one data bit was 67 ms but suggested that it could be reduced by employing more intense light.

Since liquid crystalline and amorphous solid azobenzene polymers are highly stable and can exhibit huge optical rotations and/or CD that cannot easily be attained in other systems, they show promise in both physical and optical applications. Unique applications taking advantage of the optical switching functionality are also expected.

8. Other Applications

Significant studies using photocontrollable materials other than in the ways mentioned above will now be mentioned.

Yaroshchuk and coworkers investigated three-dimensional molecular alignments in azobenzene LCPs [195,196]. Various states of optical anisotropy can be induced by photoirradiation using two-different wavelengths of polarized light, which is illustrated by three-dimensional index ellipsoid at uniaxial and biaxial in the literatures. Photocontrolled active anisotropic media might be realized for replacement of conventional electro-optic crystals. Neutron reflectometry has recently been used for investigation of photoinduced molecular reorientation inside films or bulk materials. For example, under irradiation with light to excite azobenzene molecules covalently attached to polymer matrices, neutron reflectometry measurement have been performed to investigate the nature of the photoinduced mechanical phenomenon [197].

In the field of optical communication, azobenzene-containing polymer systems are used for the development of functional elementals such as directly written waveguides with graded index [198], and an active grating coupler controlled by UV and visible light [199].

Refractive index matching/mismatching induced by controlled molecular alignment is also a versatile technology. The contrast between the clear and opaque phase within the films is a remarkable phenomenon, as shown in the literatures [162,200,201].

Biotechnology is also a suitable field for application of the photo-controllable materials. Molecular imprinted polymers (MIP) are an important technology for catching specific molecules using a polymer templated with the target molecules. Schmitzer and coworkers added photo-responsive functionalities into the polymer matrix of the MIP [202]. Target molecules can be caught and released by UV and visible light.

9. Conclusions

The applications of photocontrollable polymer materials have been extensively studied. In the present paper, the wide range of these investigations and developments were introduced and discussed based on the particular function of the photocontrollable polymer. The smart, dynamic, and straightforward characteristics of photocontrollable polymer materials are preferred in physics, mechanics, optics, photonics, materials science, and bionics. Photodriven changes in molecular alignment can play an important role in the future. The studies introduced in this paper should stimulate further developments in this area.

Acknowledgments

The authors thank Naomi Noguchi for her supporting in preparing the manuscript.

References

1. Ichimura, K. Photoalignment of liquid crystal systems. *Chem. Rev.* **2000**, *100*, 1847-1873.
2. Delaire, J.A.; Nakatani, K. Linear and nonlinear optical properties of photochromic molecules and materials. *Chem. Rev.* **2000**, *100*, 1817-1845.
3. Natansohn, A.; Rochon, P. Photoinduced motions in azo-containing polymers. *Chem. Rev.* **2002**, *102*, 4139-4175.
4. Ikeda, T.; Mamiya, J.; Yu, Y. Photomechanics of liquid-crystalline elastomers and other polymers. *Angew. Chem. Int. Ed.* **2007**, *46*, 506-528.
5. Suzuki, A.; Tanaka, T. Phase transition in polymer gels induced by visible light. *Nature* **1990**, *346*, 345-347.
6. Tatsuma, T.; Takada, K.; Miyazaki, T. UV-light-induced swelling and visible-light-induced shrinking of a TiO₂-containing redox gel. *Adv. Mater.* **2007**, *19*, 1249-1251.
7. Koshima, H.; Ojima, N.; Uchimoto, H. Mechanical motion of azobenzene crystals upon photoirradiation. *J. Am. Chem. Soc.* **2009**, *131*, 6890-6891.
8. Nakano, H. Direction control of photomechanical bending of a photochromic molecular fiber. *J. Mater. Chem.* **2010**, *20*, 2071-2074.
9. Bian, S.; Robinson, D.; Kuzyk, M.G. Optically activated cantilever using photomechanical effects in dye-doped polymer fibers. *J. Opt. Soc. Am. B* **2006**, *23*, 697-708.
10. Kobatake, S.; Takami, S.; Muto, H.; Ishikawa, T.; Irie, M. Rapid and reversible shape changes of molecular crystals on photoirradiation. *Nature* **2007**, *446*, 778-781.
11. Athanassiou, A.; Kalyva, M.; Lakiotaki, K.; Georgiou, S.; Fotakis, C. All-Optical reversible actuation of photochromic-polymer microsystems. *Adv. Mater.* **2005**, *17*, 988-992.
12. Lingyan, Z.; Al-Kaysi, R.O.; Bardeen, C.J. Reversible photoinduced twisting of molecular crystal microribbons. *J. Am. Chem. Soc.* **2011**, *133*, 12569-12575.
13. Al-Kaysi, R.O.; Bardeen, C.J. Reversible photoinduced shape changes of crystalline organic nanorods. *Adv. Mater.* **2007**, *19*, 1276-1280.
14. Eisenbach, C.D. Isomerization of aromatic azo chromophores in poly(ethyl acrylate) networks and photomechanical effect. *Polymer* **1980**, *21*, 1175-1179.

15. Wermter, H.; Finkelmann, H. Liquid crystalline elastomers as artificial muscles. *e-Polymer* **2001**, *13*, 1-13.
16. Yu, H.; Ikeda, T. Photocontrollable liquid-crystalline actuators. *Adv. Mater.* **2011**, *23*, 2149-2180.
17. Ikeda, T.; Nakano, M.; Yu, Y.; Tsutsumi, O.; Kanazawa, A. Anisotropic bending and unbending behavior of azobenzene liquid-crystalline gels by light exposure. *Adv. Mater.* **2003**, *15*, 201-205.
18. Kondo, M.; Yu, Y.; Ikeda, T. How does the initial alignment of mesogens affect the photoinduced bending behavior of liquid-crystalline elastomers? *Angew. Chem. Int. Ed.* **2006**, *45*, 1378-1382.
19. Van Oosten, C.L.; Harris, K.D.; Bastiaansen, C.W.M.; Broer, D.J. Glassy photomechanical liquid-crystal network actuators for microscale devices. *Eur. Phys. J. E.* **2007**, *23*, 329-336.
20. Yu, Y.; Nakano, M.; Ikeda, T. Miniaturizing a simple photomechanical system could expand its range of applications. *Nature* **2003**, *425*, 145.
21. Yoshino, T.; Mamiya, J.; Kinoshita, M.; Yu, Y.; Ikeda, T. Preparation and characterization of crosslinked azobenzene liquid-crystalline polymer fibers. *Mol. Cryst. Liq. Cryst.* **2007**, *478*, 989-999.
22. Camacho-Lopez, M.; Finkelmann, H.; Palffy-Muhoray, P.; Shelley, M. Fast liquid-crystal elastomer swims into the dark. *Nat. Mater.* **2004**, *3*, 307-310.
23. Yamada, M.; Kondo, M.; Miyasato, R.; Naka, Y.; Mamiya, J.; Kinoshita, M.; Shishido, A.; Yu, Y.; Barrett, C.J.; Ikeda, T. Photomobile polymer materials—Various three-dimensional movements. *J. Mater. Chem.* **2009**, *19*, 60-62.
24. Yamada, M.; Kondo, M.; Mamiya, J.; Yu, Y.; Kinoshita, M.; Barrett, C.J.; Ikeda, T. Photomobile polymer materials: Towards light-driven plastic motors. *Angew. Chem. Int. Ed.* **2008**, *47*, 4986-4988.
25. Ichimura, K.; Oh, S.K.; Nakagawa, M. Light-driven motion of liquids on a photoresponsive surface. *Science* **2000**, *288*, 1624-1626.
26. Oh, S.-K.; Nakagawa, M.; Ichimura, K. Relationship between the ability to control liquid crystal alignment and wetting properties of calix[4]resorcinarene monolayers. *J. Mater. Chem.* **2001**, *11*, 1563-1569.
27. Diguët, A.; Guillermic, R.-M.; Magome, N.; Saint-Jalmes, A.; Chen, Y.; Yoshikawa, K.; Baigl, D. Photomanipulation of a droplet by the chromocapillary effect. *Angew. Chem. Int. Ed.* **2009**, *48*, 9281-9284.
28. Loudet, J.-C.; Barois, P.; Poulin, P. Colloidal ordering from phase separation in a liquidcrystalline continuous phase. *Nature* **2000**, *407*, 611-613.
29. Nazarenko, V.G.; Nych, A.B.; Lev, B.I. Crystal structure in nematic emulsion. *Phys. Rev. Lett.* **2001**, *87*, 075504.
30. Petrov, P.G.; Terentjev, E.M. Formation of cellular solid in liquid crystal colloids. *Langmuir* **2001**, *17*, 2942-2949.
31. Yamamoto, T.; Yamamoto, J.; Lev, B.I.; Yokoyama, H. Light-induced assembly of tailored droplet arrays in nematic emulsions. *Appl. Phys. Lett.* **2002**, *81*, 2187-2189.
32. Kausar, A.; Nagano, H.; Ogata, T.; Nonaka, T.; Kurihara, S. Photocontrolled translational motion of a microscale solid object on azobenzene-doped liquid-crystalline films. *Angew. Chem. Int. Ed.* **2009**, *48*, 2144-2147.

33. Kausar, A.; Nagano, H.; Kuwahara, Y.; Ogata, T.; Kurihara, S. Photocontrolled manipulation of a microscale object: A rotational or translational mechanism. *Chem. Eur. J.* **2011**, *17*, 508-515.
34. Yablonovitch, E. Inhibited spontaneous emission in solid-state physics and electronics. *Phys. Rev. Lett.* **1987**, *58*, 2059-2062.
35. Reynolds, A.; López-Tejeira, F.; Cassagne, D.; García-Vidal, F.J.; Jouanin, C.; Sánchez-Dehesa, J. Spectral properties of opal-based photonic crystals having a SiO₂ matrix. *Phys. Rev. B* **1999**, *60*, 11422-11426.
36. Li, H.-L.; Marlow, F. Controlled arrangement of colloidal crystal strips. *Chem. Mater.* **2005**, *17*, 3809-3811.
37. Busch, K.; John, S. Photonic band gap formation in certain self-organizing systems. *Phys. Rev. E* **1998**, *58*, 3896-3908.
38. Moritsugu, M.; Kim, S.N.; Ogata, T.; Nonaka, T.; Kurihara, S.; Kubo, S.; Segawa, H.; Sato, O. Photochemical switching behavior of azofunctionalized polymer liquid crystal/SiO₂ composite photonic crystal. *Appl. Phys. Lett.* **2006**, *89*, 153131:1-153131:3.
39. Moritsugu, M.; Kim, S.-N.; Kubo, S.; Ogata, T.; Nonaka, T.; Sato, O.; Kurihara, S. Photoswitching properties of photonic crystals infiltrated with polymer liquid crystals having azobenzene side chain groups with different methylene spacers. *React. Funct. Polym.* **2011**, *71*, 30-35.
40. Kurihara, S.; Moritsugu, M.; Kubo, S.; Kim, S.-N.; Ogata, T.; Nonaka, T.; Sato, O. Photoswitching properties of photonic band gap material containing azo-polymer liquid crystal. *Eur. Polym. J.* **2007**, *43*, 4951-4960.
41. Moritsugu, M.; Shirota, T.; Kubo, S.; Ogata, T.; Sato, O.; Kurihara, S. Enhanced photochemical-shift of reflection band from an inverse opal film based on larger birefringent polymer liquid crystals: Effect of tolane group on the photochemical shift behavior. *J. Polym. Sci. Part B: Polym. Phys.* **2009**, *47*, 1981-1990.
42. Hong, J.-C.; Park, J.-H.; Chun, C.; Kim, D.-Y. Photoinduced tuning of optical stop bands in azopolymer based inverse opal photonic crystals. *Adv. Funct. Mater.* **2007**, *17*, 2462-2469.
43. Li, Y.; Deng, Y.; Tong, X.; Wang, X. Formation of photoresponsive uniform colloidal spheres from an amphiphilic azobenzene- containing random copolymer. *Macromolecules* **2006**, *39*, 1108-1115.
44. Li, Y.; Deng, Y.; He, Y.; Tong, X.; Wang, X. Amphiphilic azo polymer spheres, colloidal monolayers, and photoinduced chromophore orientation. *Langmuir* **2005**, *21*, 6567-6571.
45. Liu, J.; He, Y.; Wang, X. Azo polymer colloidal spheres containing different amounts of functional groups and their photoinduced deformation behavior. *Langmuir* **2008**, *24*, 678-682.
46. Deng, Y.; Li, N.; He, Y.; Wang, X. Hybrid colloids composed of two amphiphilic azo polymers: Fabrication, characterization, and photoresponsive properties. *Macromolecules* **2007**, *40*, 6669-6678.
47. Li, Y.; He, Y.; Tong, X.; Wang, X. Stretching effect of linearly polarized Ar⁺ laser single-beam on azo polymer colloidal spheres. *Langmuir* **2006**, *22*, 2288-2291.
48. Kamenjicki, M.; Lednev, I.K.; Asher, S.A. Photoresponsive azobenzene photonic crystals. *J. Phys. Chem. B* **2004**, *108*, 12637-12639.
49. Kamenjicki, M.; Lednev, I.K.; Mikhonin, A.; Kesavamoorthy, R.; Asher, S.A. Photochemically controlled photonic crystals. *Adv. Funct. Mater.* **2003**, *13*, 774-780.

50. Gu, Z.-Z.; Hayami, S.; Meng, Q.-B.; Iyoda, T.; Fujishima, A.; Sato, O. Control of photonic band structure by molecular aggregates. *J. Am. Chem. Soc.* **2000**, *122*, 10730-10731.
51. Kubo, S.; Gu, Z.-Z.; Takahashi, K.; Ohko, Y.; Sato, O.; Fujishima, A. Control of the optical band structure of liquid crystal infiltrated inverse opal by a photoinduced nematic-isotropic phase transition. *J. Am. Chem. Soc.* **2002**, *124*, 10950-10951.
52. Gu, Z.-Z.; Iyoda, T.; Fujishima, A.; Sato, O. Photo-reversible regulation of optical stop bands. *Adv. Mater.* **2001**, *13*, 1295-1298.
53. Kubo, S.; Gu, Z.-Z.; Takahashi, K.; Fujishima, A.; Segawa, H.; Sato, O. Tunable photonic band gap crystals based on a liquid crystal-infiltrated inverse opal structure. *J. Am. Chem. Soc.* **2004**, *126*, 8314-8319.
54. Kubo, S.; Gu, Z.-Z.; Takahashi, K.; Fujishima, A.; Segawa, H.; Sato, O. Control of the optical properties of liquid crystal-infiltrated inverse opal structures using photo irradiation and/or an electric field. *Chem. Mater.* **2005**, *17*, 2298-2309.
55. Mao, W.; Zhong, Y.; Dong, J.; Wang, H. Crystallography of two-dimensional photonic lattices formed by holography of three noncoplanar beams. *J. Opt. Soc. Am. B* **2005**, *22*, 1085-1091.
56. Zhu, X.; Xu, Y.; Yang, S. Distortion of 3D su8 photonic structures fabricated by four-beam holographic lithography with umbrella configuration. *Opt. Express* **2007**, *15*, 16546-16560.
57. Liu, Y.J.; Dai, H.T.; Sun, X.W. Holographic fabrication of azo-dye-functionalized photonic structures. *J. Mater. Chem.* **2011**, *21*, 2982-2986.
58. Ono, H.; Emoto, A.; Kawatsuki, N. Anisotropic photonic gratings formed in photocross-linkable polymer liquid crystals. *J. Appl. Phys.* **2006**, *100*, 013522:1-013522:7.
59. Emoto, A.; Ono, H.; Kawatsuki, N.; Uchida, E. Two-dimensional anisotropic gratings formed in photocrosslinkable polymer liquid crystals by multiple interference. *Jpn. J. Appl. Phys.* **2006**, *45*, 1705-1709.
60. Kawatsuki, N.; Goto, K.; Kawakami, T.; Yamamoto, T. Reversion of alignment direction in the thermally enhanced photoorientation of photo-cross-linkable polymer liquid crystal films. *Macromolecules* **2002**, *35*, 706-713.
61. Kawatsuki, N.; Fujio, K.; Hasegawa, T.; Emoto, A.; Ono, H. Surface relief formation with molecular orientation in photoreactive liquid crystalline polymer film. *J. Photopolym. Sci. Technol.* **2006**, *19*, 151-156.
62. Yu, H.; Shishido, A.; Ikeda, T. Subwavelength modulation of surface relief and refractive index in preirradiated liquid-crystalline polymer films. *Appl. Phys. Lett.* **2008**, *92*, 103117:1-103117:3.
63. Blaikie, R.J.; McNab, S.J. Evanescent interferometric lithography. *Appl. Opt.* **2001**, *40*, 1692-1698.
64. Martinez-Anton, J.C. Surface relief subwavelength gratings by means of total internal reflection evanescent wave interference lithography. *J. Opt. A: Pure Appl. Opt.* **2006**, *8*, S213-S218.
65. Ramanujam, P.S. Evanescent polarization holographic recording of sub-200-nm gratings in an azobenzene polyester. *Opt. Lett.* **2003**, *28*, 2375-2377.
66. Ohdaira, Y.; Hoshiyama, S.; Kawakami, T.; Shinbo, K.; Kato, K.; Kaneko, F. Fabrication of surface relief gratings on azo dye thin films utilizing an interference of evanescent waves. *Appl. Phys. Lett.* **2005**, *86*, 051102:1-051102:3.

67. Goldenberg, L.M.; Gritsai, Y.; Kulikovska, O.; Stumpe, J. Three-dimensional planarized diffraction structures based on surface relief gratings in azobenzene materials. *Opt. Lett.* **2008**, *33*, 1309-1311.
68. Nikolova, L.; Ramanujam, P.S. *Polarization Holography*; Cambridge University Press: Cambridge, UK, 2009.
69. Forcén, P.; Oriol, L.; Sánchez, C.; Alcalá, R.; Jankova, K.; Hvilsted, S. Pulsed recording of anisotropy and holographic polarization gratings in azo-polymethacrylates with different molecular architectures. *J. Appl. Phys.* **2008**, *103*, 123111.
70. Baldus, O.; Leopold, A.; Hagen, R.; Bieringer, T.; Zilker, S.J. Surface relief gratings generated by pulsed holography: A simple way to polymer nanostructures without isomerizing side-chains. *J. Chem. Phys.* **2001**, *114*, 1344-1349.
71. Rodríguez, F.J.; Sánchez, C.; Villacampa, B.; Alcalá, R.; Cases, R. Surface relief gratings induced by a nanosecond pulse in a liquid-crystalline azo-polymethacrylate. *Appl. Phys. Lett.* **2005**, *87*, 201914:1-201914:3.
72. Sheng, C.X.; Norwood, R.A.; Wang, J.; Thomas, J.; Wu, Y.; Zheng, Z.; Tabirian, N.; Steeves, D.M.; Kimball, B.R.; Peyghambarian, N. Time-resolved studies of photoinduced birefringence in azobenzene dye-doped polymer films. *Appl. Opt.* **2008**, *47*, 5074-5077.
73. Yager, K.G.; Barrett, C.J. Temperature modeling of laser-irradiated azo-polymer thin films. *J. Chem. Phys.* **2004**, *120*, 1089-1096.
74. Ono, H.; Nakamura, M.; Emoto, A.; Kawatsuki, N. Diffraction properties in polarization holography written by elliptical polarized light. *Jpn. J. Appl. Phys.* **2010**, *49*, 032502:1-032502:4.
75. Fukuda, T. Rewritable high-density optical recording on azobenzene polymer thin film. *Opt. Rev.* **2005**, *12*, 126-129.
76. Ono, H.; Emoto, A.; Kawatsuki, N.; Hasegawa, T. Multiplex diffraction from functionalized polymer liquid crystals and polarization conversion. *Opt. Express* **2003**, *11*, 2379-2384.
77. Ono, H.; Hatayama, A.; Emoto, A.; Kawatsuki, N.; Uchida, E. Two-dimensional crossed polarization gratings in photocrosslinkable polymer liquid crystals. *Jpn. J. Appl. Phys.* **2005**, *44*, L306-L309.
78. Galstyan, A.V.; Zakharyan, G.G.; Hakobyan, R.S. The theory of light diffraction in thin anisotropic medium. *Mol. Cryst. Liq. Cryst.* **2006**, *453*, 203-213.
79. Kuroda, K.; Matsushashi, Y.; Fujimura, R.; Shimura, T. Theory of polarization holography. *Opt. Rev.* **2011**, *18*, 374-382.
80. Sasaki, T.; Miura, K.; Hanaizumi, O.; Emoto, A.; Ono, H. Coupled-wave analysis of vector holograms: Effects of modulation depth of anisotropic phase retardation. *Appl. Opt.* **2010**, *49*, 5205-5211.
81. Oh, C.; Escuti, M.J. Time-domain analysis of periodic anisotropic media at oblique incidence: An efficient FDTD implementation. *Opt. Express* **2006**, *14*, 11870-11884.
82. Oh, C.; Escuti, M.J. Numerical analysis of polarization gratings using the finite-difference time-domain method. *Phys. Rev. A* **2007**, *76*, 043815:1-043815:8.
83. Ono, H.; Sekiguchi, T.; Emoto, A.; Kawatsuki, N. Light wave propagation in polarization holograms formed in photoreactive polymer liquid crystals. *Jpn. J. Appl. Phys.* **2008**, *47*, 3559-3563.

84. Emoto, A.; Wada, T.; Shioda, T.; Sasaki, T.; Manabe, S.; Kawatsuki, N.; Ono, H. Vector gratings fabricated by polarizer rotation exposure to hydrogen-bonded liquid crystalline polymers. *Jpn. J. Appl. Phys.* **2011**, *50*, 032502:1-032502:5.
85. Todorov, T.; Nikolova, L.; Stoyanova, K.; Tomova, N. Polarization holography. 3: Some applications of polarization holographic recording. *Appl. Opt.* **1985**, *24*, 785-788.
86. Ilieva, D.; Nedelchev, L.; Petrova, T.; Tomova, N.; Dragostinova, V.; Nikolova, L. Holographic multiplexing using photoinduced anisotropy and surface relief in azopolymer films. *J. Opt. A: Pure Appl. Opt.* **2005**, *7*, 35-39.
87. Pan, X.; Wang, C.; Wang, C.; Zhang, X. Image storage based on circular-polarization holography in an azobenzene side-chain liquid-crystalline polymer. *Appl. Opt.* **2008**, *47*, 93-98.
88. Ono, H.; Suzuki, K.; Sasaki, T.; Iwato, T.; Emoto, A.; Shioda, T.; Kawatsuki, N. Reconstruction of polarized optical images in two- and three-dimensional vector holograms. *J. Appl. Phys.* **2009**, *106*, 083109:1-083109:7.
89. Provenzano, C.; Cipparrone, G.; Mazzulla, A. Photopolarimeter based on two gratings recorded in thin organic films. *Appl. Opt.* **2006**, *45*, 3929-3934.
90. Todorov, T.; Nikolova, L.; Stoilov, G.; Hristov, B. Spectral stokesmeter. 1. Implementation of the device. *Appl. Opt.* **2007**, *46*, 6662-6668.
91. Sasaki, T.; Hatayama, A.; Emoto, A.; Ono, H.; Kawatsuki, N. Simple detection of light polarization by using crossed polarization gratings. *J. Appl. Phys.* **2006**, *100*, 063502:1-063502:4.
92. Provenzano, C.; Pagliusi, P.; Mazzulla, A.; Cipparrone, G. Method for artifact-free circular dichroism measurements based on polarization grating. *Opt. Lett.* **2010**, *35*, 1822-1824.
93. Zhou, J.; Shen, J.; Yang, J.; Ke, Y.; Wang, K.; Zhang, Q. Fabrication of a pure polarization grating in a cross-linked azopolymer by polarization-modulated holography. *Opt. Lett.* **2006**, *31*, 1370-1372.
94. Ono, H.; Emoto, A.; Takahashi, F.; Kawatsuki, N.; Hasegawa, T. Highly stable polarization gratings in photocrosslinkable polymer liquid crystals. *J. Appl. Phys.* **2003**, *94*, 1298-1303.
95. Ono, H.; Nakamura, M.; Kawatsuki, N. Conversion of circularly polarized light into linearly polarized light in anisotropic phase gratings using photo-cross-linkable polymer liquid crystals. *Appl. Phys. Lett.* **2007**, *90*, 231107:1-231107:3.
96. Emoto, A.; Fukuda, T.; Barada, D. Asymmetric polarization conversion in polarization holograms with surface relief. *Jpn. J. Appl. Phys.* **2008**, *47*, 3568-3571.
97. Yang, X.; Zhang, C.; Qi, S.; Chen, K.; Tian, J.; Zhang, G. All-optical Boolean logic gate using azo-dye doped polymer film. *Optik* **2005**, *116*, 251-254.
98. Matharu, A.S.; Jeeva, S.; Ramanujam, P.S. Liquid crystals for holographic optical data storage. *Chem. Soc. Rev.* **2007**, *36*, 1868-1880.
99. Hvilsted, S.; Sánchez, C.; Alcalá, R. The volume holographic optical storage potential in azobenzene containing polymers. *J. Mater. Chem.* **2009**, *19*, 6641-6648.
100. Saishoji, A.; Sato, D.; Shishido, A.; Ikeda, T. Formation of bragg gratings with large angular multiplicity by means of the photoinduced reorientation of azobenzene copolymers. *Langmuir* **2007**, *23*, 320-326.
101. Ishiguro, M.; Sato, D.; Shishido, A.; Ikeda, T. Bragg-type polarization gratings formed in thick polymer films containing azobenzene and tolane moieties. *Langmuir* **2007**, *23*, 332-338.

102. Minabe, J.; Maruyama, T.; Yasuda, S.; Kawano, K.; Hayashi, K.; Ogasawara, Y. Design of dye concentrations in azobenzene-containing polymer films for volume holographic storage. *Jpn. J. Appl. Phys.* **2004**, *43*, 4964-4967.
103. Forcén, P.; Oriol, L.; Sánchez, C.; Rodríguez, F.J.; Alcalá, R.; Hvilsted, S.; Jankova, K. Methacrylic azopolymers for holographic storage: a comparison among different polymer types. *Eur. Polym. J.* **2007**, *43*, 3292-3300.
104. Häckel, M.; Kador, L.; Kropp, D.; Schmidt, H.-S. Polymer blends with azobenzene-containing block copolymers as stable rewritable volume holographic media. *Adv. Mater.* **2007**, *19*, 227-231.
105. Rochon, P.; Batalla, E.; Natansohn, A. Optically induced surface gratings on azoaromatic polymer films. *Appl. Phys. Lett.* **1995**, *66*, 136-138.
106. Kim, D.Y.; Tripathy, S.K.; Li, L.; Kumar, J. Laser-induced holographic surface relief gratings on nonlinear optical polymer films. *Appl. Phys. Lett.* **1995**, *66*, 1166-1168.
107. Viswanathan, N.K.; Balasubramanian, S.; Li, L.; Tripathy, S.K.; Films, A.P. A detailed investigation of the polarization-dependent surface-relief-grating formation process on azo polymer films. *Jpn. J. Appl. Phys.* **1999**, *38*, 5928-5937.
108. Barrett, C.J.; Natansohn, A.L.; Rochon, P.L. Mechanism of optically inscribed high-efficiency diffraction gratings in azo polymer films. *J. Phys. Chem.* **1996**, *100*, 8836-8842.
109. Pedersen, T.G.; Johansen, P.M. Mean-field theory of photoinduced molecular reorientation in azobenzene liquid crystalline side-chain polymers. *Phys. Rev. Lett.* **1997**, *79*, 2470-2473.
110. Bian, S.; Li, L.; Kumar, J.; Kim, D.Y.; Williams, J.; Tripathy, S.K. Single laser beam-induced surface deformation on azobenzene polymer films. *Appl. Phys. Lett.* **1998**, *73*, 1817-1819.
111. Lefin, P.; Fiorini, C.; Nunzi, J.M. Anisotropy of the photo-induced translation diffusion of azobenzene dyes in polymer matrices. *Pure Appl. Opt.* **1998**, *7*, 71-82.
112. Barada, D.; Fukuda, T.; Itoh, M.; Yatagai, T. Numerical analysis of photoinduced surface relief formed by particle method. *Opt. Rev.* **2005**, *12*, 271-273.
113. Bellini, B.; Ackermann, J.; Klein, H.; Grave, Ch.; Dumas, Ph.; Safarov, V. Light-induced molecular motion of azobenzenecontaining molecules: A random-walk model. *J. Phys.: Condens. Matter* **2006**, *18*, S1817-S1835.
114. Juan, M.L.; Plain, J.; Bachelot, R.; Royer, P.; Gray, S.K.; Wiederrecht, G.P. Multiscale model for photoinduced molecular motion in azo polymers. *ACS Nano* **2009**, *3*, 1573-1579.
115. Viswanathan, N.K.; Kim, D.Y.; Bian, S.; Williams, J.; Liu, W.; Li, L.; Samuelson, L.; Kumar, J.; Tripathy, S.K. Surface relief structures on azo polymer films. *J. Mater. Chem.* **1999**, *9*, 1941-1955.
116. Fukuda, T.; Matsuda, H.; Shiraga, T.; Kimura, T.; Kato, M.; Viswanathan, N.K.; Kumar, J.; Tripathy, S.K. Photofabrication of surface relief grating on films of azobenzene polymer with different dye functionalization. *Macromolecules* **2000**, *33*, 4220-4225.
117. Fukuda, T.; Sumaru, K.; Yamanaka, T.; Matsuda, H. Photo-induced formation of the surface relief grating on azobenzene polymers: Analysis based on the fluid mechanics. *Mol. Cryst. Liq. Cryst.* **2000**, *345*, 263-268.
118. Kumar, J.; Li, L.; Jiang, X.L.; Kim, D.Y.; Lee, T.S.; Tripathy, S. Gradient force: The mechanism for surface relief grating formation in azobenzene functionalized polymers. *Appl. Phys. Lett.* **1998**, *72*, 2096-2098.

119. Bian, S.; Williams, J.M.; Kim, D.Y.; Li, L.; Balasubramanian, S.; Kumar, J.; Tripathy, S. Photoinduced surface deformations on azobenzene polymer films. *J. Appl. Phys.* **1999**, *86*, 4498-4508.
120. Holme, N.C.R.; Nikolova, L.; Hvilsted, S.; Rasmussen, P.H.; Berg, R.H.; Ramanujam, P.S. Optically induced surface relief phenomena in azobenzene polymers. *Appl. Phys. Lett.* **1999**, *74*, 519-521.
121. Fiorini, C.; Prudhomme, N.; De Veyrac, G.; Maurin, I.; Raimond, P.; Nunzi, J.M. Molecular migration mechanism for laser induced surface relief grating formation. *Synth. Met.* **2000**, *115*, 121-125.
122. Ikawa, T.; Mitsuoka, T.; Hasegawa, M.; Tsuchimori, M.; Watanabe, O. Optical near field induced change in viscoelasticity on an azobenzene-containing polymer surface. *J. Phys. Chem. B* **2000**, *104*, 9055-9058.
123. Landraud, N.; Peretti, J.; Chaput, F.; Lampel, G.; Boilot, J.P.; Lahlil, K.; Safarov, V.I. Near-field optical patterning on azo-hybrid sol-gel films. *Appl. Phys. Lett.* **2001**, *79*, 4562-4564.
124. Fukuda, T.; Sumaru, K.; Kimura, T.; Matsuda, H.; Narita, Y. Observation of optical near-field as photo-induced surface relief formation. *Jpn. J. Appl. Phys.* **2001**, *40*, L900-L902.
125. Fukuda, T.; Sumaru, K.; Matsuda, H.; Narita, Y.; Inoue, T.; Sato, F. Simple and effective technique for the evaluation of optical field emitted from a SNOM probe tip. *Proc. SPIE* **2002**, *4642*, 138-147.
126. Ishitobi, H.; Tanabe, M.; Sekkat, Z.; Kawata, S. Nanomovement of azo polymers induced by metal tip enhanced nearfield irradiation. *Appl. Phys. Lett.* **2007**, *91*, 091911.
127. Karageorgiev, P.; Neher, D.; Schulz, B.; Stiller, B.; Pietsch, U.; Giersig, M.; Brehmer, L. From anisotropic photo-fluidity towards nanomanipulation in the optical near-field. *Nat. Mater.* **2005**, *4*, 699-703.
128. Ubukata, T.; Seki, T.; Ichimura, T. Surface relief gratings in host-guest supramolecular materials. *Adv. Mater.* **2000**, *12*, 1675-1678.
129. Ubukata, T.; Takahashi, K.; Yokoyama, Y. Photoinduced surface relief structures formed on polymer films doped with photochromic spiropyran. *J. Phys. Org. Chem.* **2007**, *20*, 981-984.
130. Kikuchi, A.; Harada, A.; Yagi, M.; Ubukata, T.; Yokoyama, Y.; Abe, J. Photoinduced diffusive mass transfer in o-Cl-HABI amorphous thin films. *Chem. Commun.* **2010**, *46*, 2262-2264.
131. Natansohn, A.; Rochon, P. Photoinduced motions in azobenzene-based amorphous polymers: Possible photonic devices. *Adv. Mater.* **1999**, *11*, 1387-1391.
132. Ubukata, T.; Isoshima, T.; Hara, M. Wavelength-programmable organic distributed-feedback laser based on a photoassisted polymer-migration system. *Adv. Mater.* **2005**, *17*, 1630-1633.
133. Lia, X.T.; Natansohn, A.; Rochon, P. Photoinduced liquid crystal alignment based on a surface relief grating in an assembled cell. *Appl. Phys. Lett.* **1999**, *74*, 3791-3793.
134. Kim, M.H.; Kim, J.D.; Fukuda, T.; Matsuda, H. Alignment control of liquid crystals on surface relief gratings. *Liquid. Cryst.* **2000**, *27*, 1633-1640.
135. Parfenov, A.; Tamaoki, N.; Ohnishi, S. Photoinduced alignment of nematic liquid crystal on the polymer surface microrelief. *J. Appl. Phys.* **2000**, *87*, 2043-2045.

136. Chung, D.H.; Fukuda, T.; Takanishi, Y.; Ishikawa, K.; Matsuda, H.; Takezoe, H.; Osipov, M.A. Competitive effects of grooves and photoalignment on nematic liquid-crystal alignment using azobenzene polymer. *J. Appl. Phys.* **2002**, *92*, 1841-1844.
137. Ye, Y.H.; Badilescu, S.; Truong, V.V.; Rochon, P.; Natansohn, A. Self-assembly of colloidal spheres on patterned substrates. *Appl. Phys. Lett.* **2001**, *79*, 872-874.
138. Yi, D.K.; Seo, E.M.; Kim, D.Y. Surface-modulation-controlled three-dimensional colloidal crystals. *Appl. Phys. Lett.* **2002**, *80*, 225-227.
139. Yi, D.K.; Kim, M.J.; Kim, D.Y. Surface relief grating induced colloidal crystal structures. *Langmuir* **2002**, *18*, 2019-2023.
140. Watanabe, O.; Ikawa, T.; Kato, T.; Tawata, M.; Shimoyama, H. Area-selective photoimmobilization of a two-dimensional array of colloidal spheres on a photodeformed template formed in photoresponsive azopolymer film. *Appl. Phys. Lett.* **2006**, *88*, 204107:1-204107:3.
141. Fukuda, T.; Keum, C.D.; Matsuda, H.; Yase, K.; Tamada, K. Photo-induced surface relief on Azo polymer for optical component fabrication. *Proc. SPIE* **2003**, *5183*, 155-162.
142. Ubukata, T.; Hara, M.; Ichimura, K.; Seki, T. Phototactic mass transport in polymer films for micropatterning and alignment of functional materials. *Adv. Mater.* **2004**, *16*, 220-223.
143. Zettsu, N.; Ubukata, T.; Seki, T. Two-dimensional manipulation of poly(3-dodecylthiophene) using light-driven instant mass migration as a molecular conveyer. *Jpn. J. Appl. Phys.* **2004**, *43*, L1169-L1171.
144. Beck, J.S.; Vartuli, J.C. Recent advances in the synthesis, characterization and applications of mesoporous molecular sieves. *Curr. Opin. Solid State Mater. Sci.* **1996**, *1*, 76-87.
145. Beck, J.S.; Vartuli, J.C.; Roth, W.J.; Leonowicz, M.E.; Kresge, C.T.; Schmitt, K.D.; Chu, C.T.-W.; Olson, D.H.; Sheppard, E.W.; McCullen, S.B.; *et al.* A new family of mesoporous molecular sieves prepared with liquid crystal templates. *J. Am. Chem. Soc.* **1992**, *114*, 10834-10843.
146. Wan, Y.; Zhao, D. On the controllable soft-templating approach to mesoporous silicates. *Chem. Rev.* **2007**, *107*, 2821-2860.
147. Huo, Q.; Zhao, D.; Feng, J.; Weston, K.; Buratto, S.K.; Stucky, G.D.; Schacht, S.; Schüth, F. Room temperature growth of mesoporous silica fibers: A new high-surface-area optical waveguide. *Adv. Mater.* **1997**, *9*, 974-978.
148. Marlow, F.; McGehee, M.D.; Zhao, D.; Chmelka, B.F.; Stucky, G.D. Doped mesoporous silica fibers: A new laser material. *Adv. Mater.* **1999**, *11*, 632-636.
149. Schomburg, C.; Wark, M.; Rohlfing, Y.; Schulz-Ekloff, G.; Wohrle, D. Photochromism of spiropyran in molecular sieve voids: effects of host-guest interaction on isomer status, switching stability and reversibility. *J. Mater. Chem.* **2001**, *11*, 2014-2021.
150. Doshi, D.A.; Huesing, N.K.; Lu, M.; Fan, H.; Lu, Y.; Simmons-Potter, K.; Potter, B.G., Jr; Hurd, A.J.; Brinker, C.J. Optically defined multifunctional patterning of photosensitive thin-film silica mesophases. *Science* **2000**, *290*, 107-111.
151. Yang, C.M.; Cho, A.T.; Pan, F.M.; Tsai, T.G.; Chao, K.J. Spin-on mesoporous silica films with ultralow dielectric constants, ordered pore structures, and hydrophobic surfaces. *Adv. Mater.* **2001**, *13*, 1099-1102.

152. Yanagisawa, T.; Shimizu, T.; Kuroda, K.; Kato, C. Trimethylsilyl derivatives of alkyltrimethylammonium-kanemite complexes and their conversion to microporous SiO₂ materials. *Bull. Chem. Soc. Jpn.* **1990**, *63*, 1535-1537.
153. Kresge, C.T.; Leonowicz, M.E.; Roth, W.J.; Vartuli, J.C.; Beck, J.S. Ordered mesoporous molecular sieves synthesized by a liquid-crystal template mechanism. *Nature* **1992**, *359*, 710-712.
154. Tolbert, S.H.; Firouzi, A.; Stucky, G.D.; Chmelka, B.F. Magnetic field alignment of ordered silicate-surfactant composites and mesoporous silica. *Science* **1997**, *278*, 264-268.
155. Miyata, H.; Kuroda, K. Formation of a continuous mesoporous silica film with fully aligned mesochannels on a glass substrate. *Chem. Mater.* **2000**, *12*, 49-54.
156. Ichimura, K.; Fujiwara, T.; Momose, M.; Matsunaga, D. Surface-assisted photoalignment control of lyotropic liquid crystals. Part 1. Characterisation and photoalignment of aqueous solutions of a water-soluble dye as lyotropic liquid crystals. *J. Mater. Chem.* **2002**, *12*, 3380-3386.
157. Kawashima, Y.; Nakagawa, M.; Ichimura, K.; Seki, T. Photo-orientation of mesoporous silica materials via transfer from an azobenzene-containing polymer monolayer. *J. Mater. Chem.* **2004**, *14*, 328-335.
158. Kawashima, Y.; Nakagawa, M.; Seki, T.; Ichimura, K. Photo-orientation of mesostructured silica via hierarchical multiple transfer. *Chem. Mater.* **2002**, *14*, 2842-2844.
159. Yang, H.; Kuperman, A.; Coombs, N.; Mamiche-Afara, S.; Ozin, G.A. Synthesis of oriented films of mesoporous silica on mica. *Nature* **1996**, *379*, 703-705.
160. Seki, T.; Fukuda, K.; Ichimura, K. Photocontrol of polymer chain organization using a photochromic monolayer. *Langmuir* **1999**, *15*, 5098-5101.
161. Fukumoto, H.; Nagano, S.; Seki, T. *In situ* polymerization of liquid crystalline monomers within photoaligned mesoporous silica thin film. *Chem. Lett.* **2006**, *35*, 180-181.
162. Kawatsuki, N.; Kawakami, T.; Yamamoto, T. A photoinduced birefringent film with a high orientational order obtained from a novel polymer liquid crystal. *Adv. Mater.* **2001**, *13*, 1337-1339.
163. Fukumoto, H.; Nagano, S.; Kawatsuki, N.; Seki, T. Photo-orientation of mesoporous silica thin films on photocrosslinkable polymer films. *Adv. Mater.* **2005**, *17*, 1035-1039.
164. Park, M.; Harrison, C.; Chaikin, P.M.; Register, R.A.; Adamson, D.H. Block copolymer lithography: periodic arrays of ~10¹¹ holes in 1 square centimeter. *Science* **1997**, *276*, 1401-1404.
165. Sidorenko, A.; Tokarev, I.; Minko, S.; Stamm, M. Ordered reactive nanomembranes/nanotemplates from thin films of block copolymer supramolecular assembly. *J. Am. Chem. Soc.* **2003**, *125*, 12211-12216.
166. Osuji, C.; Ferreira, P.J.; Mao, G.; Ober, C.K.; Vander Sande, J.B.; Thomas, E.L. Alignment of self-assembled hierarchical microstructure in liquid crystalline diblock copolymers using high magnetic fields. *Macromolecules* **2004**, *37*, 9903-9908.
167. Morkved, T.L.; Lu, M.; Urbas, A.M.; Ehrichs, E.E.; Jaeger, H.M.; Mansky, P.; Russell, T.P. Local control of microdomain orientation in diblock copolymer thin films with electric fields. *Science* **1996**, *273*, 931-933.
168. Tomikawa, N.; Lu, Z.; Itoh, T.; Imrie, C.T.; Adachi, M.; Tokita, M.; Watanabe, J. Orientation of microphase-segregated cylinders in liquid crystalline diblock copolymer by magnetic field. *Jpn. J. Appl. Phys.* **2005**, *44*, L711-L714.

169. Hamley, I.W.; Castelletto, V.; Lu, Z.B.; Imrie, C.T.; Itoh, T.; Al-hussein, A. Interplay between smectic ordering and microphase separation in a series of side-group liquid-crystal block copolymers. *Macromolecules* **2004**, *37*, 4798-4807.
170. Tokita, M.; Adachi, M.; Takazawa, F.; Watanabe, J. Shear flow orientation of cylindrical microdomain in liquid crystalline diblock copolymer and its potentiality as anchoring substrate for nematic mesogens. *Jpn. J. Appl. Phys.* **2006**, *45*, 9152-9156.
171. Yu, H.; Iyoda, T.; Ikeda, T. Photoinduced alignment of nanocylinders by supramolecular cooperative motions. *J. Am. Chem. Soc.* **2006**, *128*, 11010-11011.
172. Morikawa, Y.; Nagano, S.; Watanabe, K.; Kamata, K.; Iyoda, T.; Seki, T. Optical alignment and patterning of nanoscale microdomains in a block copolymer thin film. *Adv. Mater.* **2006**, *18*, 883-886.
173. Tian, Y.; Watanabe, K.; Kong, X.; Abe, J.; Iyoda, T. Synthesis, nanostructures, and functionality of amphiphilic liquid crystalline block copolymers with azobenzene moieties. *Macromolecules* **2002**, *35*, 3739-3747.
174. Chen, A.; Komura, M.; Kamata, K.; Iyoda, T. Highly ordered arrays of mesoporous silica nanorods with tunable aspect ratios from block copolymer thin films. *Adv. Mater.* **2008**, *20*, 763-767.
175. Li, J.; Kamata, K.; Watanabe, S.; Iyoda, T. Template- and vacuum-ultraviolet-assisted fabrication of a Ag-nanoparticle array on flexible and rigid substrates. *Adv. Mater.* **2007**, *19*, 1267-1271.
176. Watanabe, S.; Fujiwara, R.; Hada, M.; Okazaki, Y.; Iyoda, T. Site-specific recognition of nanophase-separated surfaces of amphiphilic block copolymers by hydrophilic and hydrophobic gold nanoparticles. *Angew. Chem. Int. Ed.* **2007**, *46*, 1120-1123.
177. Watanabe, R.; Kamata, K.; Iyoda, T. Nanodimple arrays fabricated on SiO₂ surfaces by wet etching through block copolymer thin films. *Jpn. J. Appl. Phys.* **2008**, *47*, 5039-5041.
178. Li, J.; Kamata, K.; Komura, M.; Yamada, T.; Yoshida, H.; Iyoda, T. Anisotropic ion conductivity in liquid crystalline diblock copolymer membranes with perpendicularly oriented PEO cylindrical domains. *Macromolecules* **2007**, *40*, 8125-8128.
179. Huck, N.P.M.; Jager, W.F.; Lange, B.D.; Feringa, B.L. Dynamic control and amplification of molecular chirality by circular polarized light. *Science* **1996**, *273*, 1686-1688.
180. Suarez, M.; Schuster, G.B. Photoresolution of an axially chiral bicyclo[3.3.0]octan-3-one: Phototriggers for a liquid-crystal-based optical switch. *J. Am. Chem. Soc.* **1995**, *117*, 6732-6738.
181. Choi, S.W.; Ha, N.Y.; Shiromo, K.; Rao, N.V.S.; Paul, M.K.; Toyooka, T.; Nishimura, S.; Wu, J.W.; Park, B.; Takanishi, Y.; *et al.* Photoinduced circular anisotropy in a photochromic w-shaped-molecule-doped polymeric liquid crystal film. *Phys. Rev. E* **2006**, *73*, 021702:1-021702:6.
182. Vera, F.; Tejedor, R.M.; Romero, P.; Barberá, J.; Ros, M.B.; Serrano, J.L.; Sierra, T. Light-driven supramolecular chirality in propeller-like hydrogen-bonded complexes that show columnar mesomorphism. *Angew. Chem. Int. Ed.* **2007**, *46*, 1873-1877.
183. Tejedor, R.M.; Millaruelo, M.; Oriol, L.; Serrano, J.L.; Alcalá, R.; Rodríguez, F.J.; Villacampa, B. Photoinduced supramolecular chirality in side-chain liquid crystalline azopolymers. *J. Mater. Chem.* **2006**, *16*, 1674-1680.
184. Maxein, G.; Zentel, R. Photochemical inversion of the helical twist sense in chiral polyisocyanates. *Macromolecules* **1995**, *28*, 8438-8440.

185. Mayer, S.; Zentel, R. Switching of the helical polymer conformation in a solid polymer film. *Macromol. Rapid Commun.* **2000**, *21*, 927-930.
186. Angiolini, L.; Bozio, R.; Giorgini, L.; Pedron, D.; Turco, G.; Daurú, A. Photomodulation of the chiroptical properties of new chiral methacrylic polymers with side chain azobenzene moieties. *Chem. Eur. J.* **2002**, *8*, 4241-4247.
187. Nikilova, L.; Todorov, T.; Ivanov, M.; Andruzzi, F.; Hvilsted, S.; Ramanujam, P.S. Photoinduced circular anisotropy in side-chain azobenzene polyesters. *Opt. Mater.* **1997**, *8*, 255-258.
188. Nikolova, L.; Nedelchev, L.; Todorov, T.; Petrova, Tz.; Tomova, N.; Dragostinova, V.; Ramanujam, P.S.; Hvilsted, S. Self-induced light polarization rotation in azobenzene-containing polymers. *Appl. Phys. Lett.* **2000**, *77*, 657-659.
189. Iftime, G.; Lagugné-Labarthe, F.; Natansohn, A.; Rochon, P. Control of chirality of an azobenzene liquid crystalline polymer with circularly polarized light. *J. Am. Chem. Soc.* **2000**, *122*, 126646-12650.
190. Kim, M.J.; Shin, B.G.; Kim, J.J.; Kim, D.Y. Photoinduced supramolecular chirality in amorphous azobenzene polymer films. *J. Am. Chem. Soc.* **2002**, *124*, 3504-3505.
191. Sumimura, H.; Fukuda, T.; Kim, J.Y.; Barada, D.; Itoh, M.; Yatagai, T. Photoinduced chirality in azobenzene amorphous copolymer bearing large birefringent moiety. *Jpn. J. Appl. Phys.* **2006**, *45*, 451-455.
192. Fukuda, T.; Barada, D.; Sumimura, H.; Kim, J.Y.; Itoh, M.; Yatagai, T. Numerical analysis of photoinduced chirality in azobenzene polymer and its application as photoaddressable polarization altering elements. *Jpn. J. Appl. Phys.* **2008**, *47*, 1196-1202.
193. Pagés, S.; Lagugné-Labarthe, F.; Buffeteau, T.; Sourisseau, C. Photoinduced linear and/or circular birefringences from light propagation through amorphous or smectic azopolymer films. *Appl. Phys. B* **2002**, *75*, 541-548.
194. Barada, D.; Fukuda, T.; Sumimura, H.; Kim, J.Y.; Itoh, M.; Yatagai, T. Polarization recording in photoinduced chiral material for optical storage. *Jpn. J. Appl. Phys.* **2007**, *46*, 3928-3932.
195. Yaroshchuk, O.V.; Kiselev, A.D.; Zakrevskyy, Y.; Bidna, T.; Kelly, J.; Chien, L.-C.; Lindau, J. Photoinduced three-dimensional orientational order in side chain liquid crystalline azopolymers. *Phys. Rev. E* **2003**, *68*, 011803:1-011803:15.
196. Yaroshchuk, O.V.; Dumont, M.; Zakrevskyy, Y.A.; Bidna, T.V.; Lindau, J. Molecular structure of azopolymers and photoinduced 3D orientational order. 1. Azobenzene polyesters. *J. Phys. Chem. B* **2004**, *108*, 4647-4658.
197. Yager, K.G.; Tanchak, O.M.; Godbout, C.; Fritzsche, H.; Barrett, C.J. Photomechanical effects in azo-polymers studied by neutron reflectometry. *Macromolecules* **2006**, *39*, 9311-9319.
198. Karimi-Alavijeh, H.; Parsanasab, G.-M.; Baghban, M.-A.; Sarailou, E.; Gharavi, A.; Javadpour, S.; Shkunov, V. Fabrication of graded index waveguides in azo polymers using a direct writing technique. *Appl. Phys. Lett.* **2008**, *92*, 041105:1-041105:3.
199. Bang, C.-U.; Shishido, A.; Ikeda, T. Azobenzene liquid-crystalline polymer for optical switching of grating waveguide couplers with a flat surface. *Macromol. Rapid Commun.* **2007**, *28*, 1040-1044.
200. Liu, J.; Wang, M.; Li, Y.; Zhong, H. Photo-triggered assembly/disassembly of macroscopically ordered monodomain lamellar structure in side-chain liquid crystalline polymer containing strong polar azobenzene mesogens. *Liquid. Cryst.* **2011**, *38*, 105-113.

201. Kawatsuki, N.; Hasegawa, T.; Ono, H.; Yamamoto, T. Scattering linear polarizer based on a polymer blend of photo-cross-linkable polymer liquid crystal and photoinactive polymer. *Chem. Lett.* **2002**, *31*, 1256-1257.
202. Gomy, C.; Schmitzer, A.R. Synthesis and photoresponsive properties of a molecularly imprinted polymer. *Org. Lett.* **2007**, *9*, 3865-3868.

© 2012 by the authors; licensee MDPI, Basel, Switzerland. This article is an open access article distributed under the terms and conditions of the Creative Commons Attribution license (<http://creativecommons.org/licenses/by/3.0/>).